Commission of the European Communities

NEA/NSC/DOC (93) 11
INDC (EUR) 027/G

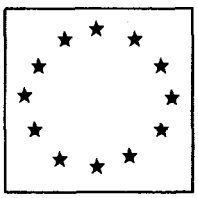

JOINT
RESEARCH
CENTRE

ANNUAL PROGRESS REPORT ON NUCLEAR DATA 1992

CENTRAL BUREAU FOR NUCLEAR MEASUREMENTS

GEEL (BELGIUM)

June 1993
EUR 15155 EN

Commission of the European Communities

NEA/NSC/DOC (93) 11
INDC (EUR) 027/G

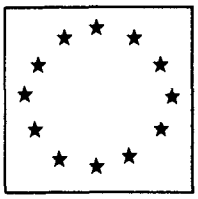

JOINT
RESEARCH
CENTRE

ANNUAL PROGRESS REPORT ON NUCLEAR DATA 1992

CENTRAL BUREAU FOR NUCLEAR MEASUREMENTS

GEEL (BELGIUM)

June 1993
EUR 15155 EN

LEGAL NOTICE

Neither the Commission of the European Communities nor any person acting on behalf of the Commission is responsible for the use which might be made of the following information

CATALOGUE N°: CD-NA-15155-EN-C *©ESC-EEC-EAEC, BRUSSELS-LUXEMBOURG, 1993*

TABLE OF CONTENTS

Note : This Annual Report is the last one being published under the name of the Central Bureau for Nuclear Measurements. In the future reports will appear under the new name

Institute
FOR
Reference Materials and Measurements
(IRMM)

For further information concerning the Project Nuclear Measurements (Nuclear Data, Nuclear Metrology), please contact A.J. Deruytter, Project Manager, IRMM, Retieseweg, B-2440 Geel, Belgium

Editor : H.H. Hansen

EXECUTIVE SUMMARY

A.J. Deruytter

In 1992 the efforts for the improvement of the set of **standard neutron cross-sections** and for other quantities selected within the INDC/NEANDC Standards File continued. In particular work on the standard cross-section ratio $^{235}U(n,f)/H(n,n)$ continued with Frisch gridded ionization chambers and using octacosanol samples as hydrogeneous layers.
A double Frisch gridded ionization chamber was used to measure mass-energy- and angular distribution of fission fragments for $^{237}Np(n,f)$ from 0.5 MeV to 5.5 MeV neutron energy.
Measurements of alpha-particle emission probabilities of ^{239}Pu showed results for the two major emissions to disagree with recent evaluated data.
Requests from the nuclear science community became more and more demanding and follow from deficiencies in available experimental data sets, which are detected by careful evaluation efforts in the framework of the International Evaluation Cooperation (IEC) of the NEA Nuclear Science Committee (NEA-NSC). The requests are summarized in the NEA High Priority Request List.
In the subproject on **nuclear data for fission technology** a measurement was performed of the normalization of the ^{239}Pu fission cross-section which solved a normalization problem of earlier Weston and Todd data of about 4 %.
Parameters for 384 resonances in ^{58}Ni and 350 resonances in ^{60}Ni have been analyzed upto 1 MeV and 800 KeV, respectively. The data were submitted for inclusion in the JEF and EFF files.
In the field of **nuclear data for fusion technology**, double differential neutron-emission cross-sections for $^{9}Be(n,2n)$ for incident neutron energies between 0.6 MeV and 11.1 MeV have been transmitted to the NEA Data Bank.
During 1992 an extensive measurement campaign has been performed on neutron emission cross-sections from ^{207}Pb.
New measurements of $^{58}Ni(n,\alpha)$ relative to the $^{27}Al(n,\alpha)$ cross-section instead of relative to H(n,n) were performed at 8 MeV neutron-energy under five angles with a ΔE-E telescope. Aim is to resolve the discrepancy of our earlier data with the ENDF/B6 evaluation.
Several more basic measurements linked to our nuclear data programme were performed mainly for PhD research and using GELINA as a high resolution neutron spectrometer unique in Europe. They concern: spin assignments of ^{238}U p-wave resonances as a contribution to parity-non-conservation (PNC) studies at Los Alamos, a search for the shape isomer in ^{239}U and ^{233}Th and the study of γ-ray decay towards the isomeric groundstate in ^{239}U, high resolution ^{138}Ba

(n,γ) measurements in view of understanding the s-process nucleosynthesis, the study of radioactive transitions from n-capture in ^{53}Cr resonances, and ^{242}Pu and ^{244}Pu mass and energy distributions and their correlations.

In the **radionuclide metrology subproject** contributions were made by the preparation of low-energy X-ray standard sources, measurements of K-shell fluorescence yields, standardization of a ^{152}Eu solution, evaluation of the second EUROMET intercomparison of ^{192}Ir brachytherapy sources, and low level measurements on volcanic rock, archeological ceramics, soil and river sediments. Impressive was the background reduction in low-level measurements with a high-purity Ge detector in the underground laboratory HADES (collaboration with SCK/CEN, Mol (B)). The technique of time-differential perturbed angular distributions (TDPAD) of γ-rays with the pulsed beam facility at the Van de Graaff was applied for identification of fluorine residence sites in silicon and germanium, as well as for radiation damage studies in GaAs.

In the area of neutron metrology fast neutron and γ-ray fluences close to the GELINA target were measured in view of damage caused by irradiations with fast neutrons at a fluence level of 10^{15} n/cm^2.

The **major facilities** of CBNM, the Geel linear electron accelerator GELINA and the 7 MV Van de Graaff accelerator were fully operational. They were used for neutron data measurements and in the non-nuclear applications. In 1992 the first phase of a refurbishment plan for GELINA was approved.

Experiments in **radiation physics** started as exploratory research were continued in 1992. Energy-spectra and angular distributions of X-ray transition radiation emitted by different radiators were obtained; an optical transition radiation system was built that delivers information about the electron energy, beam size and beam divergence, characteristics important for further work in radiation physics. A study of the Smith-Purcell effect to produce intense X-ray beams using ultrarelativistic electrons travelling close to a metallic grating is underway.

NUCLEAR DATA

NUCLEAR DATA FOR STANDARDS

The objective of the work on standard nuclear data is to improve the set of neutron data to be used in measurements consistency checks. Competing reactions, angular and kinetic energy distributions of the reaction products have to be studied to increase the reliability of the given standard cross sections. Appropriate research topics are selected from listings of the INDC/NEANDC Standards File. Complementary work is devoted to radionuclide decay data and associated atomic data requested for calibration and reference purposes.

Neutron Data for Standards

Standard Cross Section Ratio $^{235}U(n,f)/H(n,n)$

F.-J. Hambsch, R. Vogt, G. Willems*, P. Robouch, J. Van Gestel, J. Pauwels, A. Rodriguez, R. Besenthal

In continuation of this investigation[1] measurements at incident neutron energies ranging from 0.3 to 2 MeV have been performed for six different octacosanol samples. The thickness of the octacosanol layers under investigation are 136 µg/cm^2, 137 µg/cm^2, 217 µg/cm^2, 280 µg/cm^2, 353 µg/cm^2 and 550 µg/cm^2. The samples were prepared by two different evaporation runs.
Analysis of the proton-recoil spectra carried out for the first measurement series revealed a sharp distribution with an energy resolution of about 14 keV FWHM. This was deduced from the width of a high precision pulse generator peak, which was continuously connected during the experiment. The resolution is demonstrated by a fit with a Gaussian distribution to the measured pulse generator peak in Fig. 1.
Analysis of the second measurement series revealed, however, a much smoother spectral shape of the proton recoils, although the width of the pulse generator peak did not change.
A comparison of the proton recoil spectra measured for samples of 136 µg/cm^2 and 137 µg/cm^2 at about 2 MeV neutron energy at the high energy end of the spectrum is given in Fig. 2. It is obvious that the two spectra are different, which accounts to about 1 % of the total counts. If the aim is to reduce the total measurement error to about 0.5 % such a dissent is not acceptable. This also

---

* Visiting Scientist from KU Leuven, Belgium
(1) CBNM Annual Report 91, EUR 14374 EN

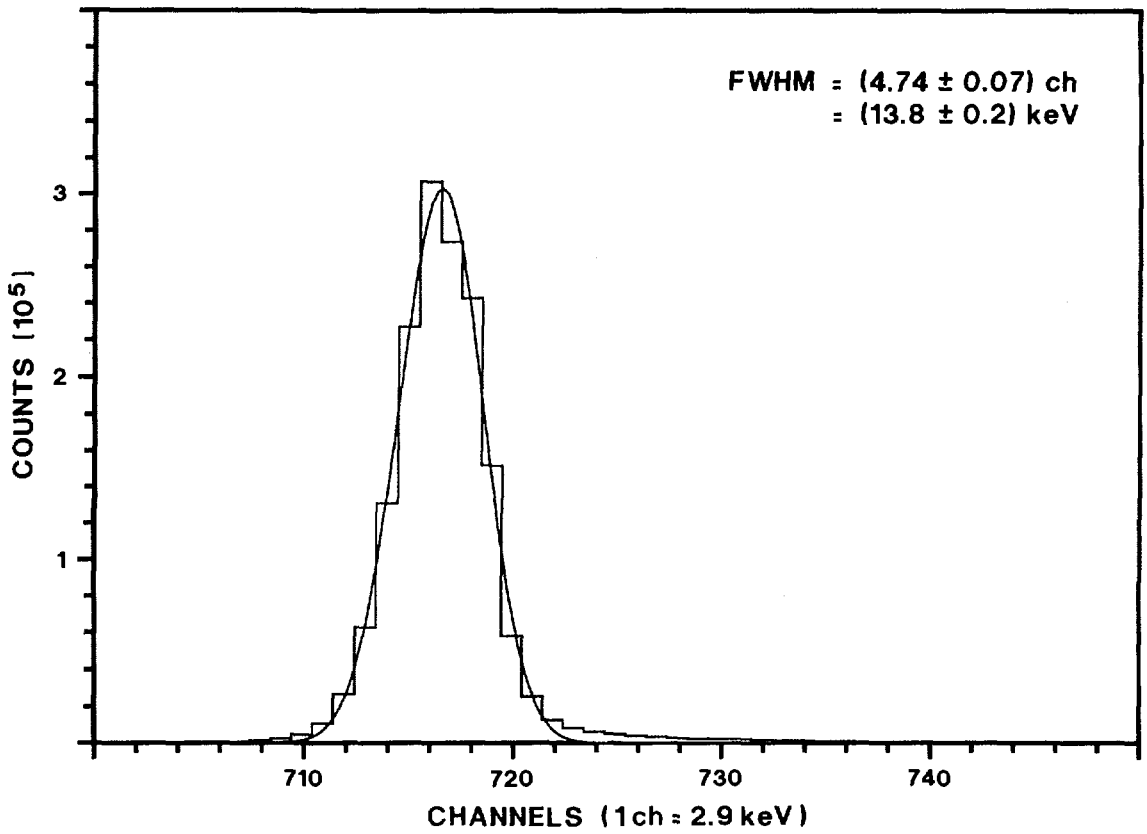

Fig. 1. Precise pulse generator peak and corresponding Gaussian fit

because the difference appears at the high energy end of the spectrum, where those events are measured which are emitted close to 0° with respect to the normal on the cathode. There the energy loss in the sample should be a minimum, if a homogeneous surface is present. However, without notice the gas supplier had changed the gas quality. Furthermore also the neutron producing target had been replaced due to a low neutron yield.

Using a certified gas with N50-quality and the former TiT-target for the neutron production resulted in the spectrum shown in Fig. 3 by a dashed line. There is still a visible discrepancy with the first measured spectrum (solid line) at the high energy end. But compared to Fig. 2 the shape has considerably improved. Because of these non reproducible measurements of the proton recoil spectra, we tried to measure and compare also the tristearin samples used in earlier experiments[1]. Up to now only the thinnest tristearin sample of 148 $\mu g/cm^2$ has been investigated. The comparison with the best octacosanol measurement is given in Fig. 4. The two distributions are very much the same. However, the tristearin distribution is obviously more extended to higher channel numbers. This is unexpected because energy loss calculations based on

(1) H.-H. Knitter, C. Budtz-Jørgensen and H. Bax, Proc. Advisory Group Meeting on Nuclear Standard Reference Data, IAEA TECDOC 335 (1985)

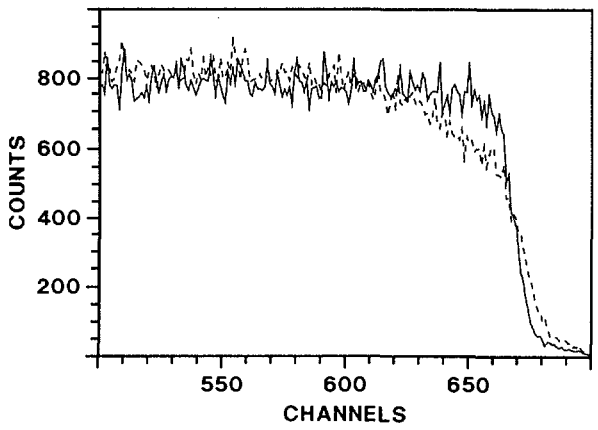

Fig. 2. Comparison of the proton recoil spectra for 2 MeV incident neutron energy and octacosanol sample thicknesses of 137 µg/cm² (solid line) and 136 µg/cm² (dashed line)

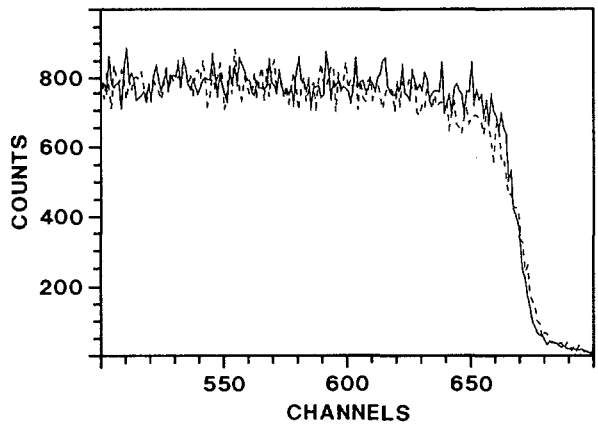

Fig. 3. Comparison of the proton recoil spectra for 2 MeV incident neutron energy and octacosanol sample thicknesses of 137 µg/cm² (solid line) and 136 µg/cm² (dashed line). Certified N50-gas and better TiT-target used

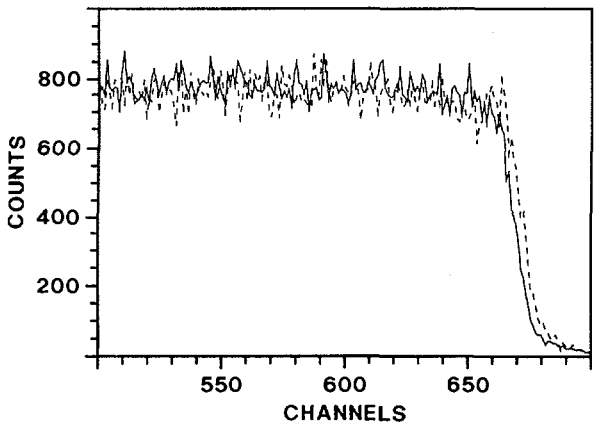

Fig. 4. Comparison of the proton recoil spectra for 2 MeV incident neutron energy and octacosanol sample of 137 µg/cm² (solid line) and tristearin sample of 148 µg/cm² (dashed line)

tables of Ziegler et al.[1] for protons of 2 MeV showed the same value of ~ 25 keV energy loss for both the tristearin sample of 148 µg/cm² and the octacosanol sample of 137 µg/cm². From this it is expected that both distributions end in the same channel. The measured difference of two to three channels, respectively 6 to 9 keV, however, seems to indicate that something might be wrong. For three different octacosanol samples of the first measurement a plot of the energy loss

(1) J. F. Ziegler et al., The stopping and range of ions in solids, Pergamon Press, New York (1985)

versus half height of the proton recoil distribution is given in Fig. 9. A straight line fit to the points gives the stopping power value for octacosanol at 2 MeV proton energy. The resulting value from the fit of 240 keV/mg/cm^2 is in disagreement to the expected value of 179 keV/mg/cm^2 [1].
To solve the existing discrepancies a new measurement series is foreseen including all the different octacosanol and tristearin samples available. To check also the influence of the neutron producing target new TiT-targets have already been ordered.

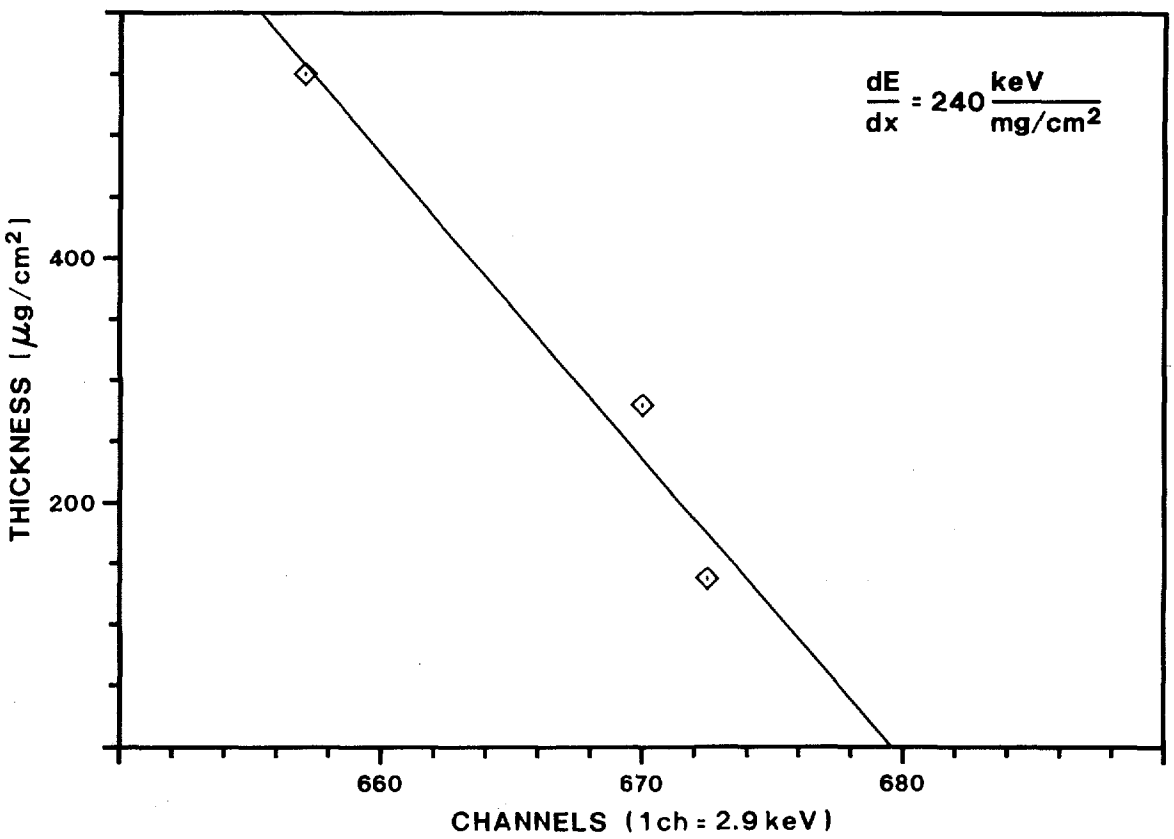

Fig. 5. ***Octacosanol sample thickness versus channel number at half height of the proton recoil distribution. Straight line fit to get the stopping power at 2 MeV incident neutron energy***

The ^{235}U Fission Fragment Anisotropies

F.-J. Hambsch

On request from the NEANDC Standards Subcommittee, which has decided to present the NEANDC/INDC Standards file as an OECD/NEA document, a review on the ^{235}U fission fragment anisotropies has been written. Since the last review in 1983[2] of the status of the measured fission fragment anisotropies as

(1) J. F. Ziegler et al., The stopping and range of ions in solids, Pergamon Press, New York (1985)

(2) S.S. Kapoor , Nuclear Data Standards for Nuclear Measurements, Technical Reports Series Nr. 227, p. 47 (IAEA, Vienna, 1983)

function of incident neutron energy in ^{235}U only a few new measurements have been performed. However, for measurements of fission cross sections which do not cover the whole 2π solid angle or for corrections of self absorption within the target for small emission angles with respect to the plane of the deposit the knowledge of the fragment angular distribution is needed. The main experimental emphasis has been devoted to the neutron energy range from 3 keV to 500 keV[1] and from 0.5 MeV to 6 MeV in steps of 0.5 MeV[2]. The main result was that the measured anisotropies in the energy range from 0.5 MeV to 6 MeV agree with the result already published, but have smaller errors. The negative anisotropies for neutron energies below 0.3 MeV measured already by several other authors have been confirmed.

Investigation of the Correlation Between Prompt Gamma-Ray Emission and Fission Fragments from $^{252}Cf(SF)$

F.-J. Hambsch, R. Vogt

Recently this type of activity has been partly restarted under different aspects. In a first instance the fission fragment signals from the used Frisch gridded ionization chamber served as input to a newly developed four parameter data acquisition system. This system connected to the SUN-SPARC based local area network made it possible to do directly data acquisition and online monitoring with LISA (LIstmode and Spectral data Analysis, see page 52 for details) based on the commercial visualization package PV-WAVE.

The four parametric listmode data were directly acquired via the SCSI-interface onto 4 mm DAT-tapes with 2 GByte capacity. Approximately $2.5 \cdot 10^8$ events have been registered up to now. Different steps of data analysis are ongoing before fission fragment mass- and total kinetic energy distributions can be calculated.

The second aim of this experiment is to check the quality of the ionization chamber, the data reduction and the spontaneous fissioning target by the achieved mass resolution in comparison to recently published data of fission fragment properties in the cold fragmentation region of $^{252}Cf(SF)$.

Furthermore in a recent investigation[3] of the correlation of fission fragments with prompt neutron emission from $^{252}Cf(SF)$ an increased yield at asymmetric fragment masses has been found. This is especially interesting to be verified because the prompt neutron database measured[3] is extremely good ($\sim 10^8$ coincident events) and inconsistencies with older prompt neutron measurements of fission fragments may become visible.

(1) F.-J. Hambsch, H.-H. Knitter, C. Budtz-Jørgensen, Proc. of the Seminar on Fission, ed. C. Wagemans, Habay-la-Neuve, 1986, BLG586
(2) Ch. Straede, C. Budtz-Jørgensen and H.-H. Knitter, Nucl. Phys. A462 (1987) 85
(3) J. van Aarle, W. Westmeier and P. Patselt, Verhandlungen der DPG 1992,p. 165

Neutron Induced Fission of ^{237}Np

P. Siegler*, F.-J. Hambsch, R. Vogt

The already mentioned measurement [1] of the fission fragment properties of the reaction $^{237}Np(n,f)$ has been started using the 7 MV Van de Graaff accelerator as a neutron source. A double Frisch gridded ionization chamber is used to measure the mass-, energy- and angular distribution of fission fragments as function of the incident neutron energy.

The fact, that ^{237}Np has a fission threshold at about 0.7 MeV neutron energy, makes an investigation in this energy region especially interesting. It has not yet been clearly proven by other experiments[2, 3] whether or not the fission fragment properties exhibit changes with incident neutron energy.

Up to now measurements at 0.5, 0.7, 1, 1.09, 1.3, 1.6, 4, 4.6, 5, 5.5 MeV neutron energy were performed. About $2 \cdot 10^5$ coincident fission events have been measured at all neutron energies except the lowest. The D(d,n) reaction has been used for neutron energies above 4 MeV and the T(p,n) for the lower energies.

In the threshold region, where finer energy steps are needed the spread in neutron energy due to energy loss of protons in the tritium target becomes severe. To reduce this spread several additional runs between 0.3 MeV and 0.7 MeV with thin lithium-fluoride targets using the $^7Li(p,n)^7Be$ reaction are planned.

A difficulty for pre-neutron mass calculations is the fact that $\bar{\nu}$, the number of prompt neutrons emitted as function of fragment mass is not known for $^{237}Np(n,f)$. Therefore the same setup has been used to measure the thermal neutron induced fission of ^{235}U. The results will serve as a reference for the analysis of the ^{237}Np data because for $^{235}U(n_{th},f)$ all the distributions of the different fission fragment parameters are well known. The target dimensions were similar to those of the neptunium target and therefore the necessary corrections to the raw data can be compared and adapted. The large fission cross section for $^{235}U(n_{th},f)$ allowed a short measuring period of two days only with a total number of $2 \cdot 10^6$ events.

Another very important fact which has to be taken into account is the pulse height defect in gases like the used 90 % Ar 10 % CH_4. Calculations for the pulse height defect of fission fragments in the energy and mass range covered, have been started using a computer code based on the energy loss tables of Ziegler et al.[4].

---

* EC Fellow from Technical University Darmstadt, Germany

(1) CBNM Annual Report 91, EUR 14374 EN
(2) B. D. Kuzminov et al., Sov. Jour. Nucl. Phys. 11(1970)166
(3) R. Müller et al., Phys. Rev. C29(1984)885
(4) J. F. Ziegler et al., The stopping and range of ions in solids, Pergamon Press, New York (1985)

The calculations concerning the multi-modal random neck-rupture model of Brosa, Grossmann and Müller[1] have been completed. The existence of the so-called standard channels as well as the superlong channel could be established. Complete data sets for every fission channel with all the shape parameters as well as the binding energies are available. Fig. 6 displays the results of the channel search for the compound nucleus ^{238}Np. The channels are drawn as function of the half length l and the neck radius r of the corresponding shape of the nucleus.

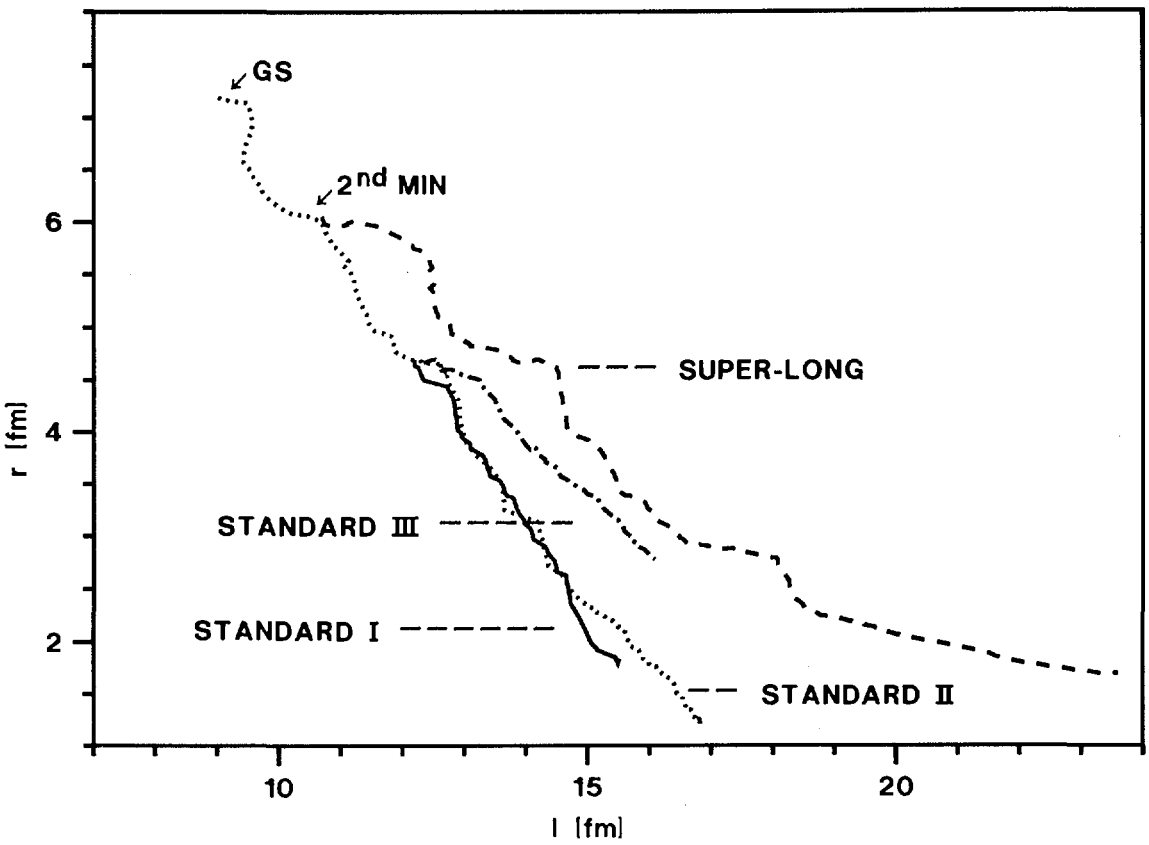

Fig. 6. ***Projection of the fission channels to the plane represented by the choosen parametrization of the nucleus***

In the second minimum the first bifurcation takes place and the superlong channel starts. Following the standard channel after the second barrier another bifurcation exists where the splitting into the three standard channels occurs. The end of each standard channel represents a prescission configuration which is associated within the random neck-rupture model to certain fission properties. The prescission configuration of the superlong channel is deduced from the minimum in Fig. 7 for E_{gs}-E_{def} at l = 21 fm.

(1) U. Brosa et al., Phys. Reports 197(1990)167

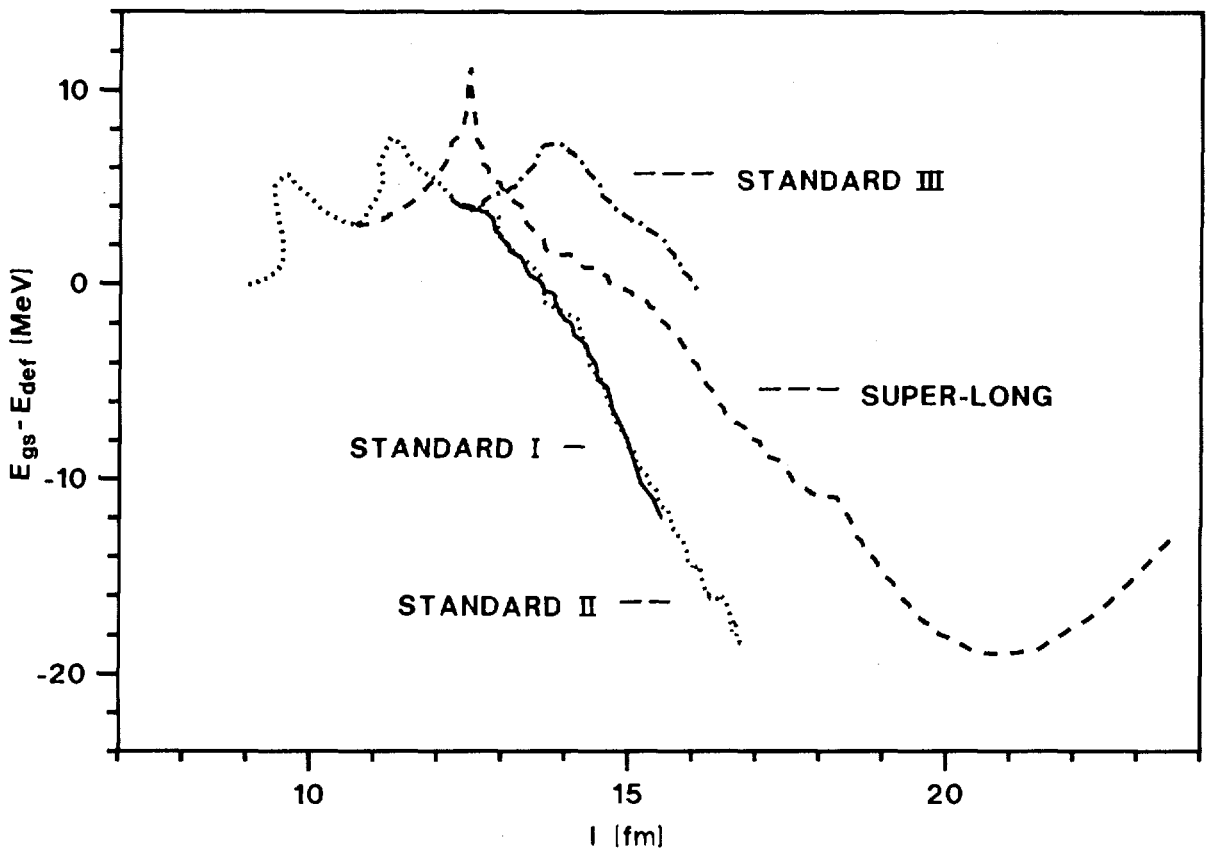

Fig. 7. ***Potential energy E_{gs}-E_{def} of the deformed nucleus for the different fission channels as function of the elongation parameter l***

Table 1. ***Pre-scission parameters and deduced fission fragment properties for each fission channel***

	E^*_S [MeV]	B [MeV]	ΔU [MeV]	V_{cou} [MeV]	$-V_{nuc}$ [MeV]	TKE [MeV]	σ_{TKE} [MeV]	A	σ_A	Z	σ_Z	V_{mul}	l [fm]	Δl [fm]	TOTL [fm]	r [fm]	z [fm]
STANDARD I	6,6	7,5	17,7	223,0	32,9	189,8	9,6	135,4	3,4	52,9	1,3	1,92	15,5	4,2	29,2	1,8	0,3
STANDARD II	9,3	7,5	24,7	207,1	28,1	178,6	9,6	139,1	5,5	54,4	2,1	3,33	16,8	5,5	31,6	1,2	0,7
STANDARD III	2,3	7,4	6,1	196,7	30,3	173,0	6,1	153,7	3,2	60,0	1,3	1,72	16,1	2,3	30,2	2,8	2,2
SUPERLONG	9,3	10,9	24,7	174,8	18,2	155,0	10,0	119,0	13,0	46,5	5,1	7,12	21,0	8,5	39,4	2,0	0,2

From Fig. 6 and Fig. 7 it is obvious that standard I and II are difficult to be separated. However, by comparing the calculated mass splits based on the full set of shape parameters it was possible to assign calculated points to the different channels. Special is also the standard III channel with its third barrier and the early ending. It is interesting to see if this component influences the experimental results.

The predictions of the fission properties of the individual channels equivalent to the components of fission given in Table 1 are now possible.

The $^{10}B(n,\alpha)\ ^{7}Li$ Cross Section

E. Wattecamps

On request of the INDC/NEANDC nuclear standards subcommittee the status of the $^{10}B(n,\alpha)\ ^{7}Li$ standard cross section was collated in a paper submitted for publication as an OECD/NEA document. The report covers the following topics:

- status of the requests;
- status of the recommended reference data;
- status of recent and ongoing measurements.

Non-Neutron Data for Standards

Alpha-Particle Emission Probabilities (P_α) of ^{239}Pu

E. García-Toraño*, M. Aceña*, G. Bortels, D. Mouchel

The P_α of 16 transitions were measured and analysed at CBNM and CIEMAT. A solution of 99.994 % enriched ^{239}Pu (by activity) was provided for this purpose by NIST, USA. Both laboratories measured and analyzed the spectra using their own computer code. The results for the two major emissions disagree with recent evaluated data[1]. Final results for the five most important emissions only are shown in Table 2.

Table 2. Selected P_α of ^{239}Pu, measured at CBNM and CIEMAT as compared with evaluated data

Present Measurements		NDS[1]			
$P_\alpha \cdot 100$		$P_\alpha \cdot 100$		E_α [keV]	
.047	(13)	0.030	(4)	5055.35	(14)
.078	(8)	0.036	(4)	5076.29	(14)
11.94	(7)	11.5	(8)	5105.5	(8)
		< 0.03		5111.2	(2)
17.11	(14)	15.1	(8)	5144.3	(8)
70.77	(14)	73.3	(8)	5156.59	(14)
		0.03		5156.66	(20)

* Centro de Investigaciones Energéticas, Medioambientales y Tecnológicas (CIEMAT), Madrid, Spain

(1) M.R. Schmorak, Nuclear Data Sheets 66 (1992) 839

NUCLEAR DATA FOR FISSION TECHNOLOGY

The objective of the work on nuclear data for fission technology is to reach a more accurate knowledge of data requested in fission research and in fission technology. Measurements cover actinide fission cross section data as well as structural material neutron interaction data. Research topics are taken to fulfil European demands collected in the NEA High Priority Request List.

Neutron Data of Actinides

Fission Cross-Section of ^{239}Pu

C. Wagemans*, P. Van Uffelen**, A. Deruytter, R. Barthélémy, J. Van Gils

A good knowledge of the $^{239}Pu(n,f)$ cross-section is required for various applications in nuclear industry (e.g. fast reactors, MOX-fuel elements). Despite the large number of $\sigma_f(E)$-measurements for ^{239}Pu, the uncertainty on this quantity remains too important. This is mainly due to the fact that the high resolution measurements of Weston and Todd[1] in the neutron energy region from 20 eV to 100 keV are systematically lower (by about 4 %) than all recent evaluations (ENDF-B6, JEF-2, JENDL-3) and almost all other experimental data.

To tackle this problem, a NEACRP/NEANDC International Evaluation Cooperation Subgroup was created. The present work is one of the actions decided by the subgroup. Its aim is not to deliver a new set of $\sigma_f(E)$-data, but to determine a reliable value for

$$I_f = \int_{100\,eV}^{1000\,eV} \sigma_f(E)dE,$$

since Weston and Todd[1] normalized their measurements on $I_f = 8996$ b·eV.

This value was determined from a separate measurement going down to thermal neutron energy, but with fairly poor statistics. As a consequence, the uncertainty on this integral is rather important: 1.9 % normalization uncertainty, about 1 % systematic uncertainty and 0.15 % statistical uncertainty.

In order to verify the suspicion of a too low normalization factor in the Weston and Todd[1] data, two independent experiments were performed at two 8 m flight-paths of GELINA, the accelerator being operated at a 100 Hz repetition frequency with 11 ns burst widths and with an average electron current of 8 μA.

---

* Rijksuniversiteit Gent, Belgium
** Vrije Universiteit Brussel, Belgium

(1) L. Weston and J. Todd, Nucl. Sci. Eng. 88 (1984) 567

In both cases the neutron flux was determined via the detection of the $^{10}B(n,\alpha)^{7}Li$ reaction products emitted after neutron bombardment of thin ^{10}B layers.

The first experiment was performed in a low detection geometry, using two 30 cm^2 large surface barrier detectors placed outside the neutron beam for the detection of the $^{239}Pu(n,f)$ fission fragments and the $^{10}B(n,\alpha)^{7}Li$ reaction products. These detectors were placed in a large evacuated detection chamber, in the centre of which a $^{239}PuF_3$ and a ^{10}B layer were mounted back-to-back. The ^{10}B layer had a thickness of 10.2 $\mu g/cm^2$ and an isotopic enrichment of 94 % ^{10}B. The $^{239}PuF_3$ layer contained 106 μg $^{239}Pu/cm^2$; the isotopic enrichment of the plutonium used was 99.9774 % of ^{239}Pu. It is clear that absorption and self-absorption effects are very small with such layer thicknesses.

For the second measurement, a double gridded ionization chamber was used, operated with a very pure CH_4 flow as counting gas, so here the detection geometry was almost 2π. The ^{239}Pu and ^{10}B layers were mounted back-to-back on the cathode. The $^{239}PuF_3$-layer thickness was 186 $\mu g/cm^2$ (isotopic enrichment: 99.9774 % ^{239}Pu). The ^{10}B-layer thickness was 10.5 $\mu g/cm^2$, with an isotopic enrichment of 94 % ^{10}B.

In both experiments, the background was determined using the black resonances of cadmium, rhodium, tungsten, cobalt and manganese. A separate measurement was performed to check the background due to neutrons from overlapping burst by operating GELINA at a repetition frequency of 50 Hz. In another test, the not-beam-dependent background was measured by operating GELINA at a 100 Hz repetition frequency but with zero power.

Both experiments were performed in parallel. After digitizing the detector signals, bi-dimensional pulse-height versus time-of-flight spectra were stored in two HP 1000 data acquisition systems. In Fig. 8 the $^{10}B(n,\alpha)$ and $^{239}Pu(n_{th},f)$ counting rate spectra as a function of the neutron energy are shown for the measurement with the ionization chamber.

The data reduction was done adopting the ENDF-B6 values for the $^{10}B(n,\alpha)$ and the $^{239}Pu(n_{th},f)$ cross sections, the latter one being used for the normalization of the σ_f data. Combining the results of both measurements, a weighted value I_f = (9250 ± 100) b·eV was obtained, in perfect agreement with the result of an independent experiment recently performed by Weston et al., yielding I_f = (9300 ± 110) b·eV, indicating that the old Weston and Todd data should be renormalized, which will remove the major part of the discrepancy.

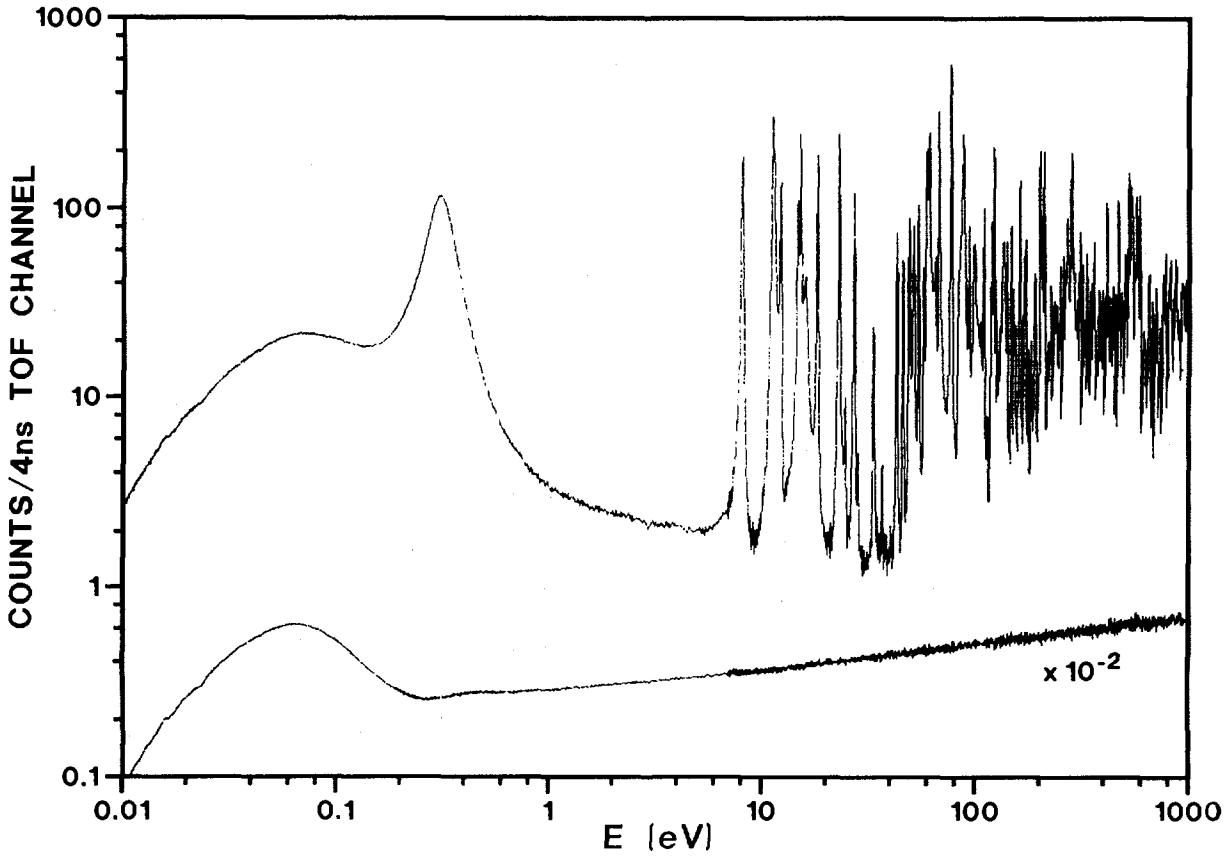

Fig. 8. *^{10}B (n,α) (lower) and ^{239}Pu(n,f) (upper) counting rate spectra as a function of the neutron energy*

Investigation of the Characteristics of the ^{242}Pu and ^{244}Pu(SF)-Fragments Distributions

C. Wagemans*, L. Dematté**, S. Pommé***, A. Deruytter, R. Barthélémy, J. Van Gils

In the frame of a systematic study of the mass and energy distributions (and their correlations) of the spontaneously fissioning plutonium isotopes, more than 30.000 ^{242}Pu(SF) events have been recorded. The measurements were performed relative to the well-known ^{239}Pu(n_{th},f) reaction, for which purpose a thermal neutron beam of the BR1 reactor of the SCK/CEN(Mol) was used. These data are being analysed, giving special attention to cold fission events.
In the case of ^{244}Pu about 7.000 spontaneous fission events have been recorded so far. These measurements are being continued.

* Rijksuniversiteit Gent, Belgium
** EC Fellow from University of Bologna, Italy
*** EC Fellow from University of Gent, Belgium

A Multi-Purpose Charged Particle Detection System

C. Wagemans*, S. Druyts**, R. Barthélémy, J. Van Gils

A multi-purpose charged particle detection system consisting of two gridded gas-flow ionization chambers and two 2000 mm^2 large, 1000 µm thick surface barrier detectors and the corresponding data acquisition system have been further developed and optimized.

In its simpliest configuration (using only one gridded ionization chamber), the $^{35}Cl(n,p)^{35}S$ and $^{36}Cl(n,p)^{36}S$ reactions have been studied from thermal up to 10 keV neutron energy. The $^{35}Cl(n,p)$ results obtained at 8 and 30 m flight-path lengths are shown in Fig. 9 and compared with the data of Koehler[1]. The resolution in our experiments is definitely better; the resonance strengths however agree within the uncertainties quoted.

By combining each ionization chamber with the corresponding surface barrier detector, a double ΔE-E telescope is formed, enabling the identification of light charged particles. In this configuration, the detector is suited for ternary fission studies.

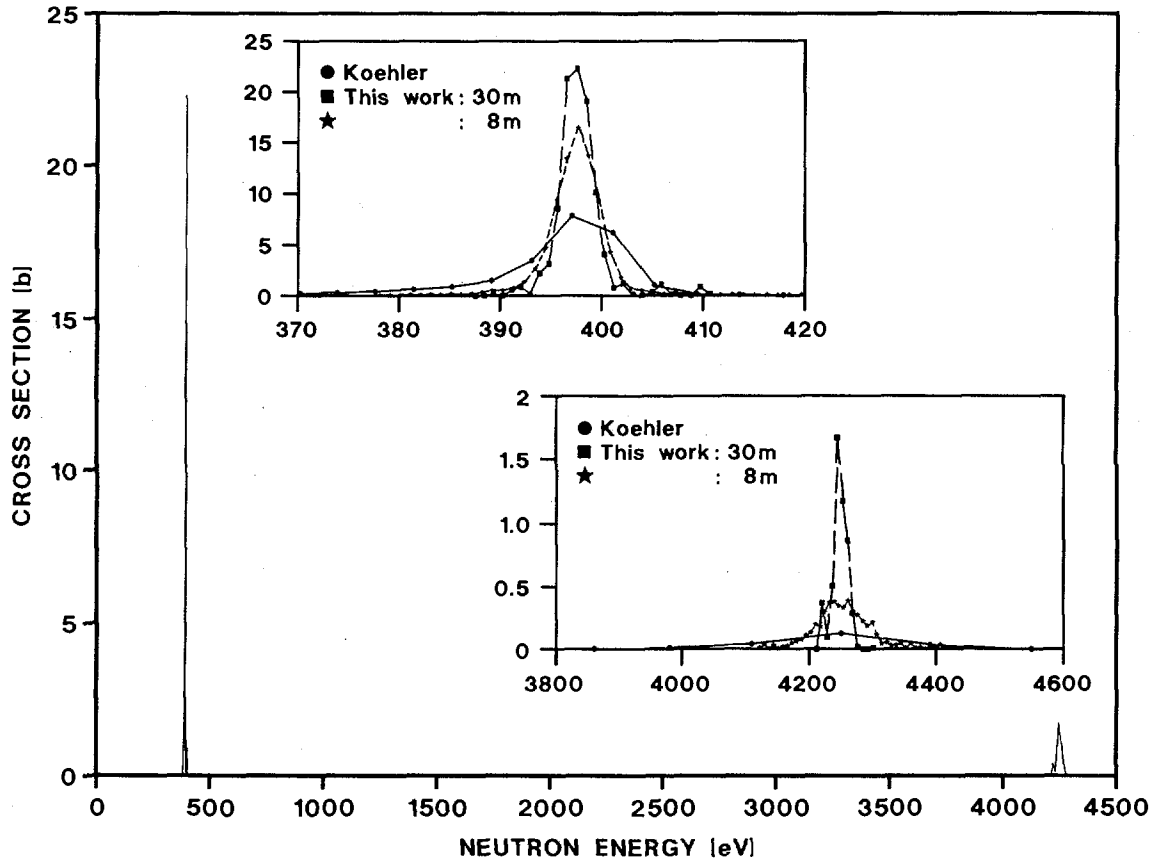

Fig. 9. ***$^{35}Cl(n,p)$ cross section versus neutron energy. The magnified inserted drawings show the results obtained for the 398 eV and 4250 eV resonances***

---

* Rijksuniversiteit Gent, Belgium
** EC Fellow from KU Leuven, Belgium
(1) P.E. Koehler, Phys. Rev. C44 (1991) 1675

Search for the Shape Isomer in ^{239}U and ^{233}Th

S. Oberstedt*, H. Weigmann, H. Wartena, C. Bürkholz, J.P. Theobald**

In the past a series of shape isomers in actinide nuclei with $Z \geq 94$ were found all decaying via the fission channel. For the lighter actinides ($Z < 94$) only a few examples exist, where the shape isomer could be detected. However, in this mass region the cross sections show intermediate structure phenomena in subthreshold fission. The interpretation in terms of the double humped fission barrier leads to discrepancies with the results from calculations on fast-fission data, especially in uranium. Therefore it has been proposed to interprete intermediate structure in $^{238}U(n, f)$ as delayed fission through a shape isomeric state with a half-life of a few ns[1]. In order to search for this reaction path, the 721.6 eV-neutron resonance in ^{239}U was investigated in a γ-γ coincidence experiment performed at the time of-flight spectrometer GELINA.

In ^{233}Th a weak indication exists for a shape isomeric state with a half-life $T_{1/2}$ of about 10 ns[2, 3], but no measurable subthreshold fission cross-section exists below $E_n < 50$ keV. Therefore, with the same experimental set-up the neutron resonances in ^{233}Th for $E_n < 4.2$ keV were investigated in order to search for intermediate structure in the relative delayed γ-ray yield.

The data-taking has now been completed. In the next two paragraphs the new experimental findings will be compared with existing systematics on isomeric half-lives and barrier parameters.

a) Is there isomeric fission in ^{239}U?

The analysis of the coincidence spectrum of the 721.6 eV-resonance (Fig. 10 left part) does not show any significant contribution of delayed coincidences stemming from isomeric fission. Testing the line-fitting procedure by simulating the coincidence spectrum with a Monte Carlo technique on the basis of theoretical assumptions on the resonance parameters shows that a shape isomer with a half-life between 1 and 10 ns must be excluded.

To be more sensitive to longer half-lives, additionally the relative delayed γ-ray yield R, i.e. the ratio between the resonances areas for delayed and prompt coincidences, was investigated. As shown in the right part of Fig. 10 the 721.6 eV resonance behaves significantly different compared to its neighbour s-wave resonances, which show apparent delayed γ-ray yield due to accidental coincidences. However, the observed difference is primarily due to the detection of fission neutrons by the detector. True delayed γ-rays from a shape isomer with a half-life $T_{1/2} < 250$ ns should show a clearly larger effect and can be excluded. This result does not depend on the assumption of either the case of

---

* EC Fellow from Technische Hochschule Darmstadt, Germany
** Technische Hochschule Darmstadt, Germany

(1) J.E. Lynn, Proc. Int. Conf. 50 years with Nuclear Fission, Vol. I, p. 148 (1990)
(2) J. Schirmer et al., Jahresbericht des MPI für Kernphysik Heidelberg, 1988, p. 67
(3) P. Reiter et al., GSI Scient. Report, 1990, p. 25

delayed fission or prompt fission and isomeric γ-ray decay back to the first potential minimum.

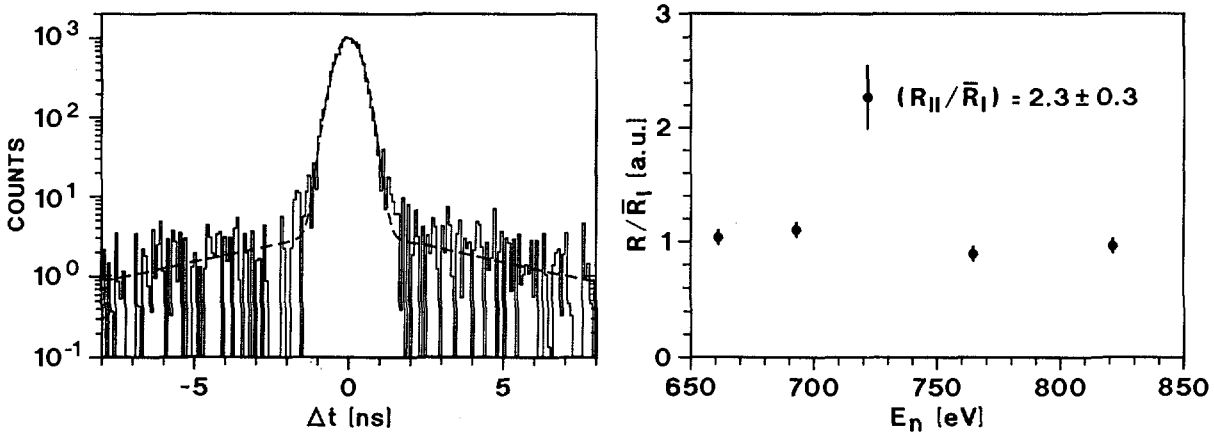

Fig. 10. In the left part the coincidence spectrum of the 721.6 eV-resonance in ^{239}U is shown. The dashed line indicates the result of fitting the data with a Gauss+exponential function. The right part gives the relative delayed γ-ray yield R in units of the average value R_I

On the basis of the experimental results the assumption that intermediate structure in the subthreshold fission cross-section of ^{238}U is caused by isomeric fission cannot be sustained. Moreover, this result may be seen as an indication that the usual parametrization of the fission barrier in terms of parabolic segments is not valid generally.

b) Intermediate structure and the shape isomer of ^{233}Th.

In Fig. 11 the distribution of the relative delayed γ-ray yield R as a function of neutron energy E_n for resonances in $^{232}Th + n$ is displayed. The left part shows the data including all γ-ray energies. The data in the right part were obtained by setting different conditions on both the first and the second γ-ray energy. The visible structures produced by larger R-values at 1 keV and 2 keV in both distributions were statistically tested against the hypothesis of a normal distribution. Including the non-statistically distributed positions for the increased R-values, a probability of less than 10^{-4} (right part of Fig. 11) was found for the hypothesis of no structure, thus indicating the existence of two class-II states in ^{233}Th in this energy range. From the shape of these structures the class-II level spacing D_{II}, the isomeric ground state energy E_{II}, the coupling width $\Gamma\downarrow$ and, in the framework of the picket-fence model, the maximum class-II fraction c_{II} could be estimated (Table 3). A further analysis of the data using the parameters from Table 3 shows that the isomeric half-life $T_{1/2}$ should lie between 1 ns and 100 ns. From the experimental values on $\Gamma\downarrow$ and $T_{1/2}$ the parameters of the inner barrier (E_A, $\hbar\omega_A$) could be estimated (Table 4). These parameters seem to fit into the global trend as it might be seen in Table 4.

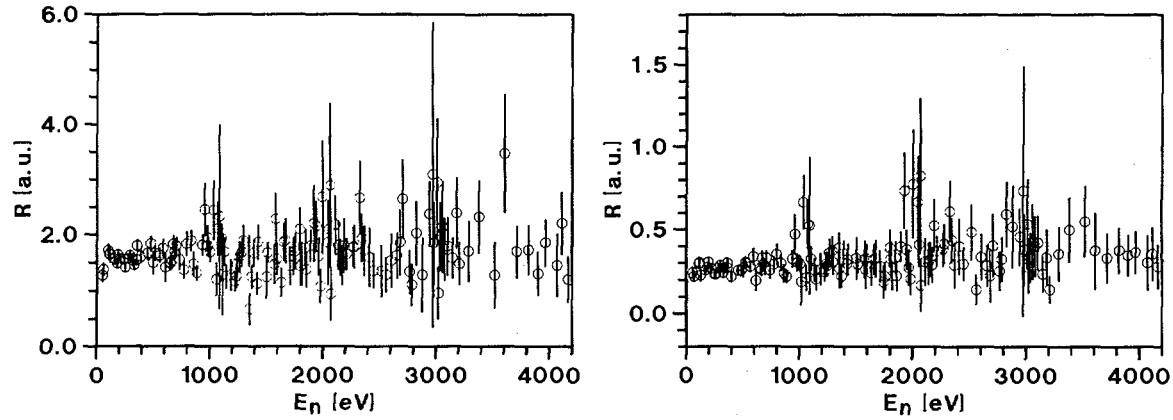

Fig. 11. Relative delayed γ-ray yield as a function of incident neutron energy E_n. The left part shows the data without γ-ray energy conditions. For the data in the right part the following γ-ray energy regions were selected: $E_{\gamma 1}$ ε (2.0,3.5) MeV and $E_{\gamma 2}$ ε (0.4, 2.9) MeV

Table 3. Experimentally obtained intervals for the class-II level spacing D_{II}, the isomeric groundstate energy E_{II}, the coupling width $\Gamma\downarrow$ and the maximum class-II admixture c_{II}

D_{II}	[keV]	0.6	2.1
E_{II}	[MeV]	1.6	2.1
$\Gamma\downarrow$	[meV]	60	200
c_{II}		0.16	0.05

Table 4. Estimate of the inner barrier parameters E_A, $\hbar\omega_A$ of ^{233}Th. For comparison the value of $\hbar\omega_A$ for two additional nuclei were calculated

Comp. Nucl.	E_{II} [MeV]	E_A [MeV]	$T_{1/2}$ [ns]	$\hbar\omega_A$ [MeV]
^{233}Th	1.85 ± 0.25	$4.7^{+0.8}_{-0.1}$	1 ... 100	$1.2^{+0.2}_{-0.1}$
^{236}U	2.35[a)] 2.56[a)]	5.6[b)] 5.7[b)]	115[a)] 240[a)]	1.26 1.16

a) p. 45 and b) p. 30 of C. Wagemans (Editor), The Nuclear Fission Process, CRC Press (1991)

Neutron Data of Structural Materials

Total Cross Section Measurements of Natural Iron

K. Berthold*, G. Rohr, C. Nazareth

A series of high resolution neutron total cross section measurements through several thicknesses of natural iron have been started. Two first transmission measurements with a running time of 10 days each for the sample thickness of 16 mm and 48 mm have been performed. These measurements result in a much better resolution than previous transmission data.
To measure the complete spectrum of neutron energy originated by the 1 ns burst of electrons impinging on a uranium target, a plastic scintillator detector (2.5 cm thick) is linked to the Nuclear Data 9900 data acquisition system to record events in two 64 k channels energy spectra of 1 ns/channel. At a 400 m distance of the detector from the neutron target the neutron energy range is recorded from 175 keV to 25 MeV.
Another measurement with a rather thick sample of 140 mm is ongoing and will be used to check whether the total cross section is responsible for the underestimation of fast neutron transmission through steel structures such as reactor pressure vessels.
It is planned to analyse the resonance structure up to 1 MeV. The resulting resonance parameter data will enable a systematic investigation of the statistical description of the cross section in the higher MeV region. In addition the underlying statistical properties of resonance parameters will be studied with respect to intermediate structure and/or non-statistical effects of the level density.

Neutron Resonance Parameters of ^{58}Ni+n and ^{60}Ni+n From Very High Resolution Transmission Measurements

A. Brusegan, R. Shelley, G. Rohr, E. Macavero, C. Van der Vorst

This work is part of the investigation of neutron cross sections of structural materials. Descriptions of the several measurements performed and initial analyses can be found in the two previous annual reports.
In order to supplement the 50, 100, 200 and 400 m flight-path data previously obtained with the 1 ns burst width of GELINA a new measurement of the neutron transmission through a 1.5 mm thick enriched sample of ^{58}Ni was done at 100 m with a 6 mm thick lithium glass detector.
The complete data sets have now been re-analysed and extended up to neutron energies of 1.01 MeV for ^{58}Ni and 800 keV for ^{60}Ni, taking into account the improved description of the resolution function of the present GELINA neutron

* EC Fellow from Technische Hochschule Darmstadt, Germany

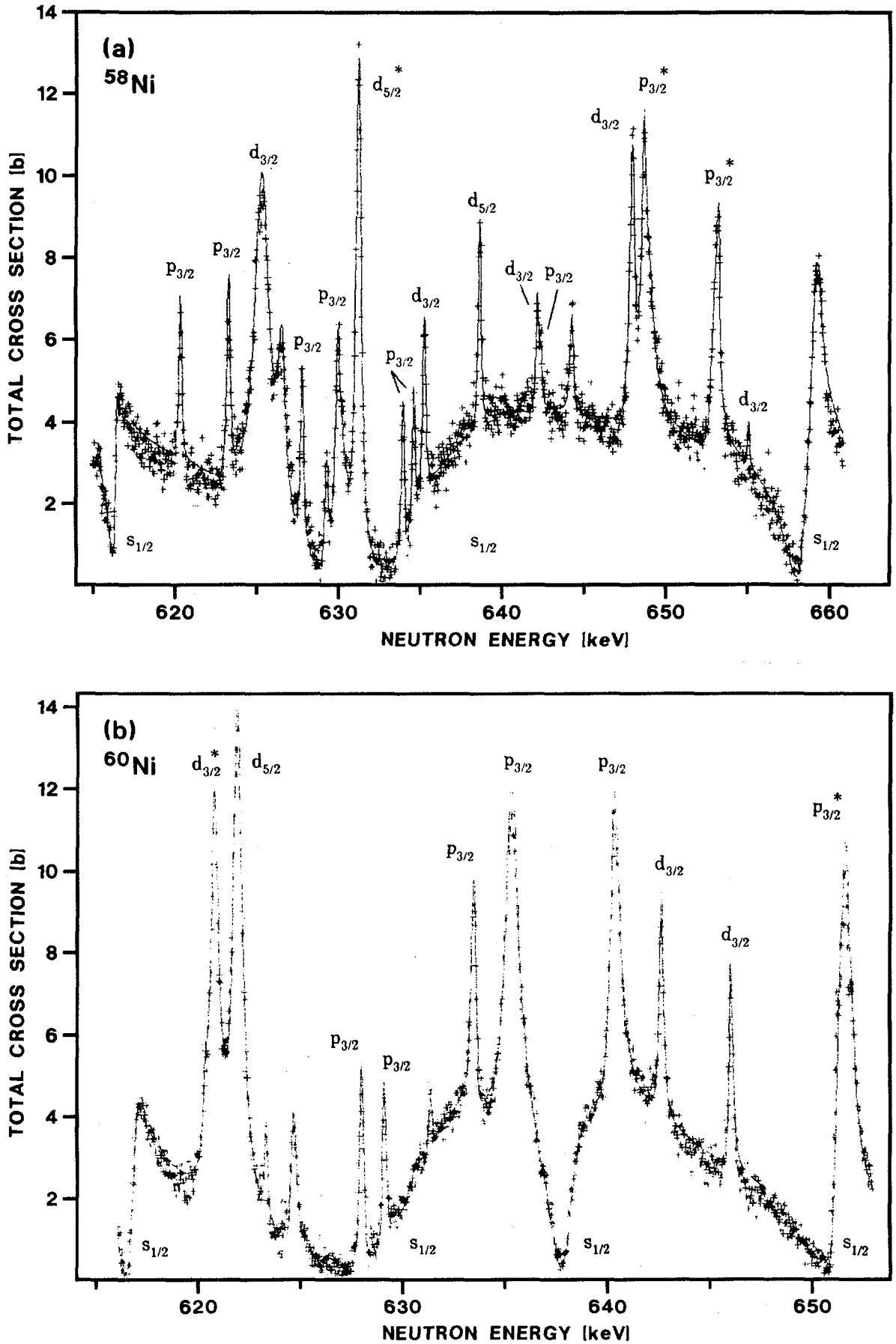

Fig. 12. *^{58}Ni (a) and ^{60}Ni (b) total neutron cross sections measured in the energy range 615 to 660 keV and fitted with our final resonance parameter data set. Spin assignments of the resonances are shown except for small levels which are assumed $p_{1/2}$ (*doublet)*

source configuration.
For the resonance parameter analysis the codes REFIT[1] and MULTI[2] have been used, the latter being recently extensively modified to accomodate the new resolution function distributions for the neutron source, with and without moderator, and for the detectors (boron slab and lithium glass). Parameters for 384 resonances in ^{58}Ni and 350 resonances in ^{60}Ni have been sent to KFK, where the collection of data required for the joint European and fusion files, JEF/EFF is coordinated.
Fig. 12 shows a small part of the measured cross section data fitted with our final resonance parameter data sets for typical mid-energy regions. The spectra show the best energy resolution presently available and was recorded at a neutron flight path of 400 m in 1 ns channels. For each isotope total cross section data for 35000 energy points in the range 0.5 - 15 MeV have been sent to the NEA data bank.

Radiative Transitions From Neutron Capture in ^{53}Cr Resonances

C. Coceva*

A measurement was performed of gamma-ray spectra emitted after neutron capture in s- and p-wave resonances of ^{53}Cr in the range 2 - 70 keV. The studied decay scheme concerns 38 levels of ^{54}Cr, with excitation energies from 0 up to 5.6 MeV. New information is obtained on the multiplicity of gamma cascades, on the spin and parity of ^{54}Cr levels, and on the spin of neutron resonances of ^{53}Cr.
Partial E1 and M1 radiative widths are obtained for transition energies from 4.1 to 9.7 MeV. Their frequency distributions follow chi-square functions with $\nu(E1) = 1.6$ and $\nu(M1) = 1.7$ degrees of freedom.
The overall energy behaviour of E1 reduced widths is in rough agreement with a Lorentzian shape, but the average intensity is higher than expected from photo-neutron data. The measured average E1 strength is $\langle S(E1)\rangle = (8.1 \pm 0.8)\cdot 10^{-15}$ MeV^{-5}. Fluctuations around this average are non-random, showing the existence of an intermediate structure. Reduced E1 widths are strongly correlated with the reduced neutron widths in the whole energy interval. Although with less evidence, an indication was found for a correlation between reduced E1 widths and spectroscopic factors of ^{54}Cr levels.
The measured average M1 strength $\langle k(M1)\rangle = (5.7 \pm 0.8)\cdot 10^{-9}$ MeV^{-3} appears to be energy-independent as in the single particle model. Reduced M1 widths exhibit wide random fluctuations. No significant correlation is found between E1 and M1 strengths.

---

* Visiting Scientist from ENEA, Bologna, Italy
(1) M.C. Moxon, AEA-In Tec-0630 and CBNM/ST/90-131/1
(2) G.F. Auchaupaugh, Report CA-5473-MS (1974)

NUCLEAR DATA FOR FUSION TECHNOLOGY

The objective of the work on nuclear data for fusion technology is to contribute to an improved knowledge of data for neutron transport calculation in the blanket and for an estimate of the gas production. Measurements are presently done in three areas: (1) double-differential neutron emission cross sections; (2) double-differential charged particle emission cross sections and (3) total and radiative capture cross sections of structural materials; since the latter are related to fission as well as to fusion technology, they are described in the section on fission technology.

Double-Differential Neutron-Emission Cross-Sections

J.A. Wartena, H. Weigmann, C. Bürkholz

The experimental methods applied as well as the main steps in the data analysis have been described in the preceding annual report.

The analysis of the data on the ^{9}Be(n,2n) cross section has been completed. In this analysis multiple scattering corrections are included which take into account the approximate angular distributions of the emitted neutrons as obtained from the preliminary analysis of the same experimental data. The final double-differential neutron emission cross sections for incident neutron energies between 1.6 and 11.1 MeV have been transmitted to the NEA data bank.

During 1992 an extensive measurement campaign has been performed on neutron emission cross sections from ^{207}Pb. Apart from the neutrons also γ rays emitted after inelastic scattering have been recorded by the NE-213 detectors

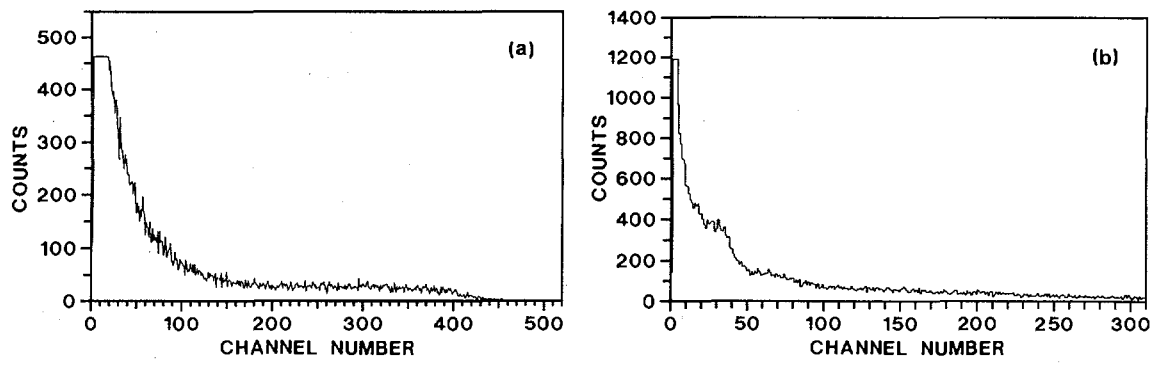

Fig. 13. ***Pulse height distributions measured by NE-213 detector for (a) neutrons and (b) γ-rays emitted from ^{207}Pb for incident neutrons between 7.7 and 8.4 MeV energy***

using pulse shape discrimination techniques. An example of the raw experimental data is shown in Fig. 13. It shows, for incident neutron energies between 7.7 and 8.4 MeV, the pulse height distributions measured by the detector which is positioned at an angle of 40 degrees with respect to the incident neutron beam; Fig. 13(a) is for emitted secondary neutrons. Fig. 13(b) for γ rays. Analysis of these data is in progress.

Correction Programmes for Multi-Parameter Data of the ΔE-E-T Telescope

G. Rollin, E. Wattecamps

A light ion telescope was designed to measure (n,x) cross-section data at the pulsed Van de Graaff accelerator (burst width of 400 ps). To be particle specific and to separate well foreground from background reactions the energy loss, the energy and the time of flight of the particles are determined. To this end six parameters of each event are measured, called E_1, E_2, T, Z, D and Y, which are respectively:

- two pulse height spectra, E_1 and E_2, and one timing pulse T from the photomultipliers viewing the pilot-U scintillator (E detector);
- one time of flight information, Z, from the Multi-Wire-Parallel-Plate-Avalanche-Counter (MWPPAC) to the pilot U scintillator;
- one pulse height spectrum, D, of the MWPPAC (ΔE detector); and
- one time of flight information, Y, from the pick-up electrode in front of the target to the pilot U scintillator.

A sequence of programs was written in C language for use at the SUN computer with the following purposes:

- correction for time dispersion in the pilot-U scintillator: typically time resolution improvement from 1000 ps down to 300 ps;
- correction for pulse height dispersion in pilot-U scintillator due to attenuation of light: typically energy resolution improvement from 37 % down to 28 %;
- transformation of light output scale into particle energy scale for particle energies from 1.5 to 9 MeV. Calibration points together with an analytical fit are shown in Fig. 14;
- correction for energy loss in the telescope from the sample to the pilot-U scintillator (38 cm distance) across three zones of isobutane and across four foils of the MWPPAC;
- correction for time delays in the observed time of flight from the sample to the pilot U scintillator (38 cm) due to the energy losses mentioned before.

The corrections are illustrated in Fig. 15 showing two-dimensional spectra of time of flight versus alpha particle energy for Ni(n,α) at 8 MeV neutron energy.

Spectrum "A" is a distribution of observed time of flight, corrected for dispersion in the scintillator, versus light output which is also corrected for dispersion in

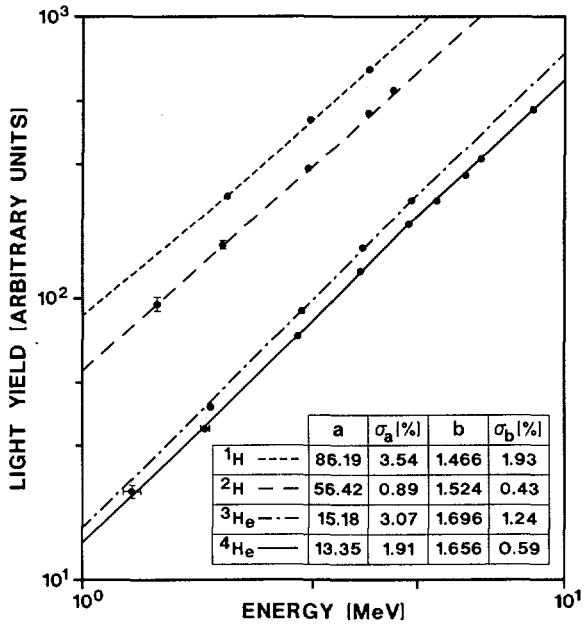

Fig. 14. Light yield produced in pilot U scintillator by various particles. Fitting equation: $Y = a \cdot E^b$

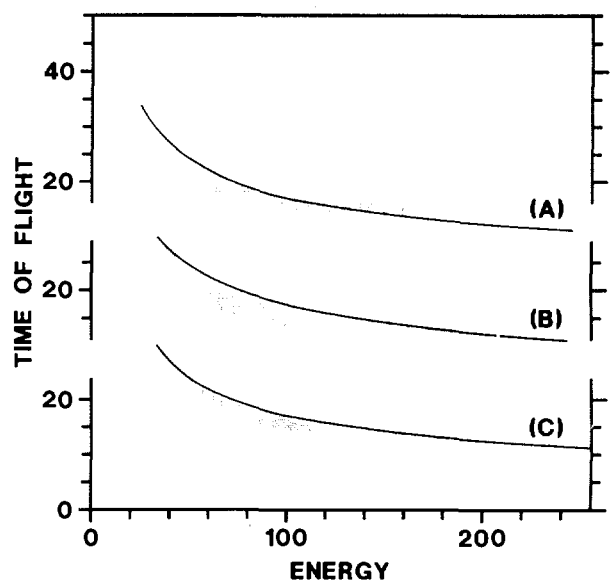

Fig. 15. Measured two-dimensional spectra of time of flight versus energy for Ni(n, α) reaction at 8 MeV neutron energy. (A) Observed time of flight versus light output. (B) Observed time of flight versus energy. (C) Time of flight versus energy, corrected for energy loss in the telescope

the scintillator. This spectrum is quite different from the expected dependence time of flight ~ $1/\sqrt{E}$.

Spectrum "B" shows time of flight versus alpha particle energy.

Spectrum "C" shows time of flight versus alpha particle energy both corrected for the effects of energy loss. It agrees well in shape and in absolute terms with the $1/\sqrt{E}$ dependence of the time of flight.

Test of Prompt Alpha Particle Detection from the ^{27}Al(n,α) Reaction

G. Rollin, C. Tsabaris*, E. Wattecamps

Measurements of (n,α) cross-section data were made in the past at the Van de Graaff relative to the well known cross section of H(n,n)H. Results for nickel, copper and their separated isotopes, were presented at the International

* EC Fellow from the University of Athens, Greece

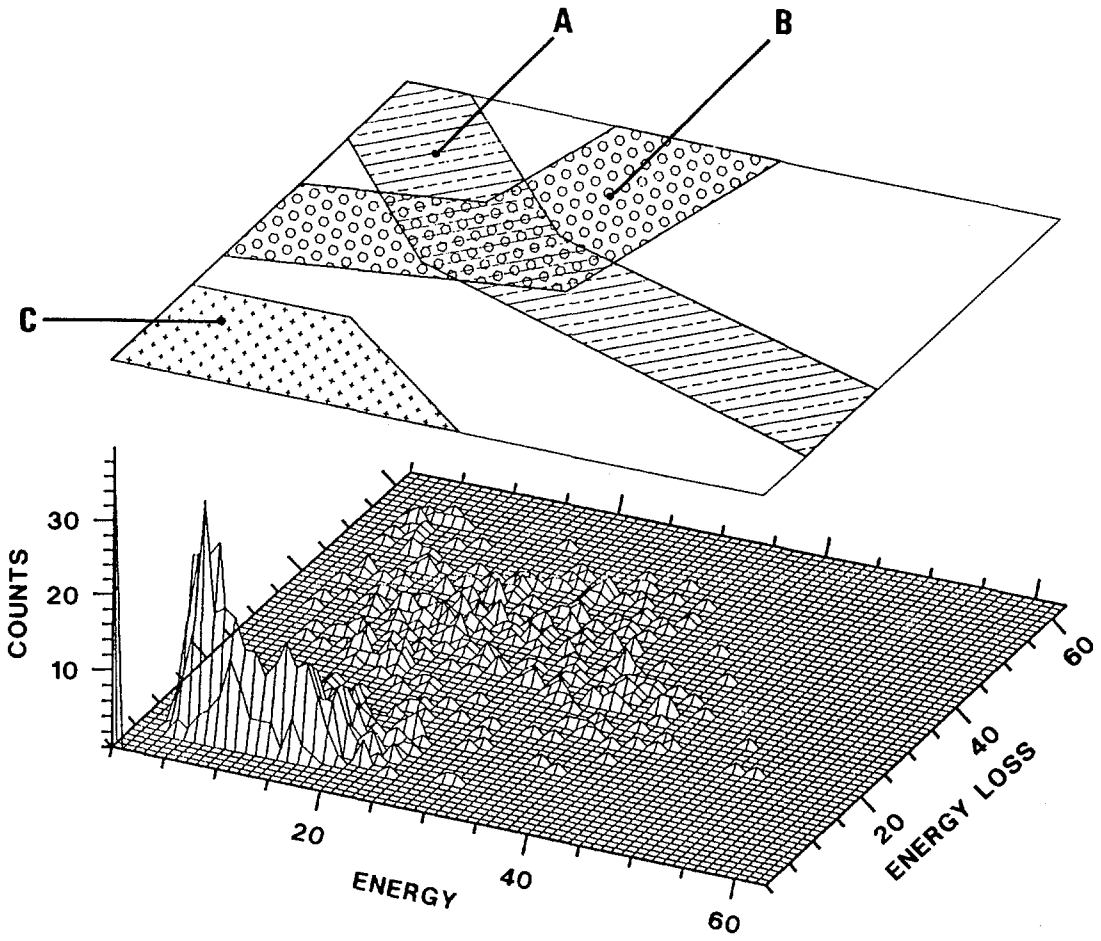

Fig. 16. ***Two dimensional spectrum of energy and energy loss observed from $^{27}Al(n,\alpha)$ with neutrons of 8 MeV during 3 hours at 2 μA beam current***

Conference on Nuclear Data for Science and Technology, Jülich, 1991. Recent Ni(n,α) data are much lower than those of the ENDF-B evaluation. Recent and older experimental data from the CBNM, and data from other laboratories as well, scatter by more than one standard deviation. Therefore, new measurements of $^{58}Ni(n,\alpha)$ relative to $^{27}Al(n,\alpha)$ are in progress, using the five angles ΔE-E telescope.

To check whether the well known activation cross section of the $^{27}Al(n,\alpha)$ reaction can be used as a reference cross section for prompt alpha particle detection, the alpha particle energy spectrum of the $^{27}Al(n,\alpha)$ reaction with neutrons of 8 MeV has been determined.

The foreground for $^{27}Al(n,\alpha)$ and the background were observed by the telescope under 51 degrees. The background is the limiting factor especially at the low energy side of the alpha particle spectrum. It could be shown that the spectrum is measurable by the ΔE-E telescope down to the lowest alpha particle energy present (0.5 MeV).

A typical foreground two-dimensional spectrum of energy loss ΔE versus energy E of alpha particles of ^{27}Al at 8 MeV neutron energy is shown in Fig. 16. Three areas can be identified:

- area A: alpha particles from $^{27}Al(n,\alpha)$, with the typical energy dependence of dE/dX versus energy;
- area B: alpha particles from ^{28}Si, with opposite energy dependence of dE/dX versus energy. It is explained by alpha particles crossing the telescope in the opposite direction (up stream, from surface barrier detector (E) to proportional counter (ΔE)) and not separable from down stream alpha particles by coincidence conditions as broad as 1 μs;
- area C: protons and less ionising radiation.

The background in the common part of areas A and B was measured with a tantalum sample at the site of the aluminium. A typical alpha particle energy spectrum of foreground and background is shown in Fig. 17. The foreground to background ratio is 3 : 1. As net signal the difference between aluminium minus the tantalum data within area A was taken.

A measurement of the reaction rate ratio of $^{58}Ni(n,\alpha)$ versus $^{27}Al(n,\alpha)$ with five telescopes, thus covering the entire angular range, is in preparation.

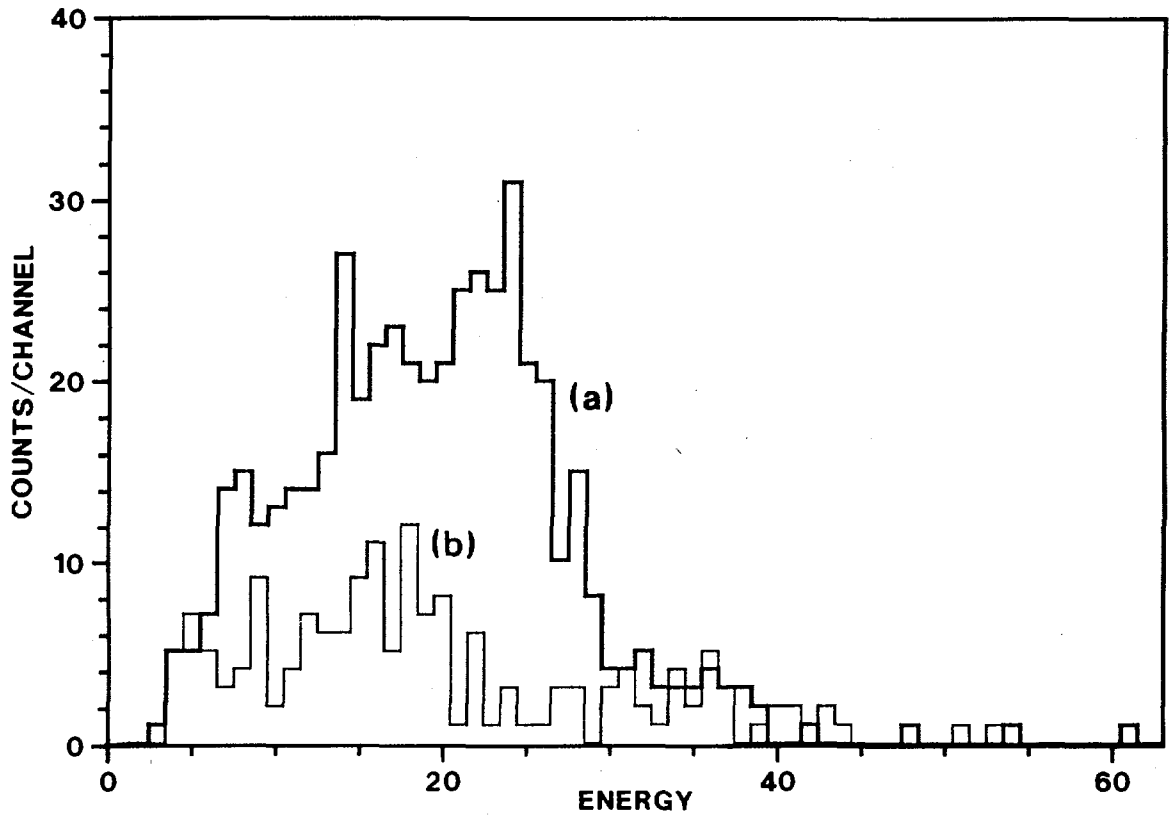

Fig. 17. Alpha particle energy spectrum for particles pertaining to area A in the ΔE - E spectrum for a measuring time of 3 hours. (a) for $^{27}Al(n,\alpha)$ or foreground, (b) for tantalum or background

Total Neutron Cross-Section Measurement of ^{27}Al at High Energy

R. Shelley, G. Rohr, C. Nazareth, M. Moxon*

A study of the neutron cross section of ^{27}Al is relevant to the structural material data required for reactor and fusion studies and recent progress made with the investigation of resonance spacings and their distribution. For this isotope no new data has become available for almost two decades and, with the present very high resolution capabilities of GELINA, the energy resolution compared to earlier measurements has been improved by an order of magnitude.
This has been achieved by measuring, at a distance of 400 m, the transmission of the neutron beam from the linac uranium target using the time-of-flight (TOF) technique. With the 1 ns pulsed linac operating at 800 Hz, the transmission through a 99.5 % pure aluminium sample (0.19293 at/b thick) was detected by a NE110 plastic scintillator viewed by four RCA photomultipliers. The resultant TOF spectra were stored in 64 k channels of 1 ns width and covered a neutron energy range from 175 keV to 25 MeV.

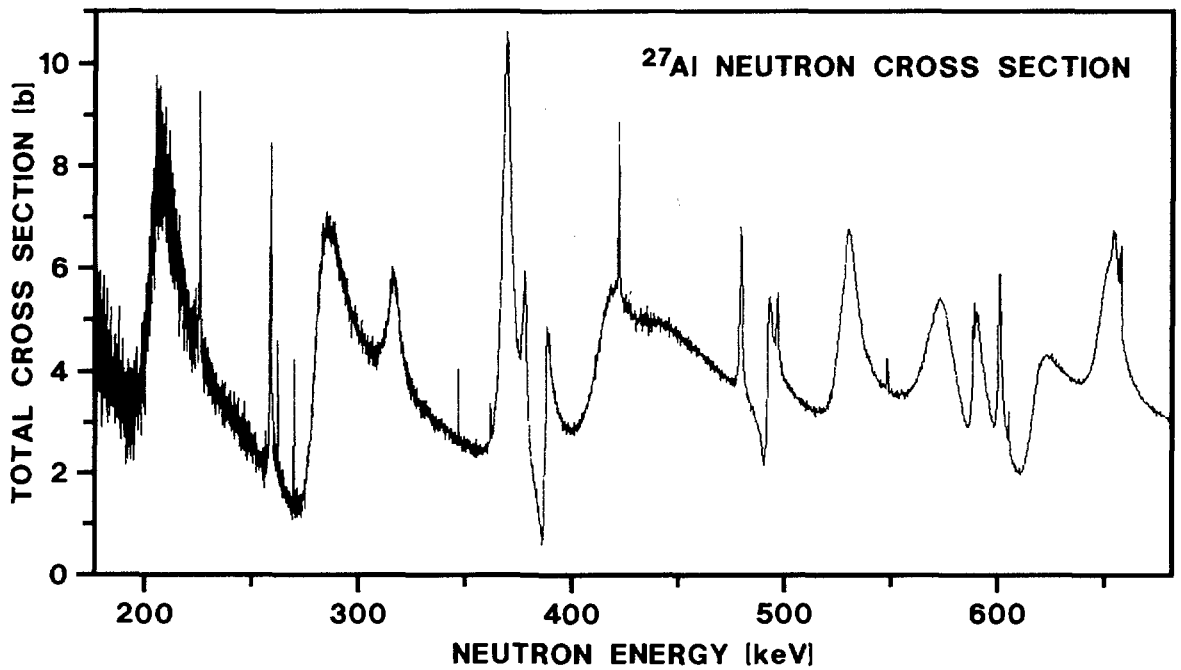

Fig. 18. *^{27}Al total neutron cross section in the energy range 180 to 680 keV. (measured data available with 1 ns/channel but presented with 8 ns/channel for ease of viewing)*

The data reduction to correct the transmission data for background and dead time effects has been completed and the cross section spectra are now available. Fig. 18 shows the complexity of the resonance structure in the cross section even when the 1 ns data have been crunched by a factor of eight. At higher energies

* Visiting Scientist from AEE, Harwell, United Kingdom

this complexity increases dramatically, the threshold for inelastic scattering is at 844 keV, and the resonance parameter analysis, which is presently at a very preliminary stage, will therefore be restricted to the energy range below 1 MeV.

SPECIAL STUDIES

Spin Assignment of ^{238}U p-Wave Resonances

F. Gunsing*, F. Corvi, H. Postma**, K. Athanasopoulos, A. Mauri***

The aim of this experiment is to contribute to parity-non-conservation (PNC) studies, performed at Los Alamos in the frame of the TRIPLE collaboration. In fact, polarized neutron measurements carried out at the LANSCE facility allowed the investigation of sixteen ^{238}U p-wave resonances and the discovery of parity mixing in a number of them(1). For the interpretation of these data, the spin of the relevant resonances is needed.

The employed method exploits the fact that the population of the low-lying levels of the compound nucleus ^{239}U formed in neutron capture depends significantly on the initial spin. These relative populations of the levels are determined by looking at the intensities of gamma transitions de-exciting them. The spin effect is then enhanced by measuring the intensity ratio of two transitions de-exciting levels of different spins. The most promising combination is the ratio of the intensity of the ground state transition de-exciting the $J^\pi = 5/2^-$ state at 539.3 keV and the intensity of the unresolved doublet consisting of the 552.1 and 554.1 transitions de-exciting states with $J^\pi = 3/2^-$ and $1/2^+$, respectively.

A measurement carried out in 1991 suffered from an important background due to the presence of 2000 ppm ^{235}U impurity. The measurement was repeated in 1992 using a uranium disc of 11.1 cm diameter and 694 g mass on loan from ORNL, containing only 9 ppm of ^{235}U. The time-of-flight capture spectra of the two runs are compared in Fig. 19 for the neutron energy range 8 - 88 eV. The structure present in the first run (upper part) due to ^{235}U resonances disappears in the second run.

From the 1992 measurements values of the ratio r = I(539)/(I(552) + I(554)) were calculated and plotted vs neutron energy as shown in Fig. 20. In spite of the large errors, a split into two groups whose average values are shown by dotted lines can be deduced. The higher group is associated with $J^\pi = 3/2^-$ in view of the larger relative population of the $5/2^+$ level at 539 keV.

In the high energy part of the γ-ray spectrum the primary transitions to the ground state and/or to the 194 keV level (both having $J^\pi = 5/2^+$) for five p-waves could be observed: clearly these resonances have $J^\pi = 3/2^-$. The preliminary spin assignments obtained with the low-level population method and with the primary transitions are summarized in Table 5. The results of the two methods

---

* EC Fellow from Technical University of Delft, The Netherlands
** Visiting scientist from Technical University of Delft, The Netherlands
*** National expert from ENEA, Bologna, Italy
(1) X. Zhu e.al., Phys. Rev. V 46 (2), 1992, p. 768

are in good agreement. The longitudinal asymmetry values P of the Los Alamos group are listed in the last column of Table 5. With the exception of the 10.2 eV resonance, these data are consistent with the present spin assignment.

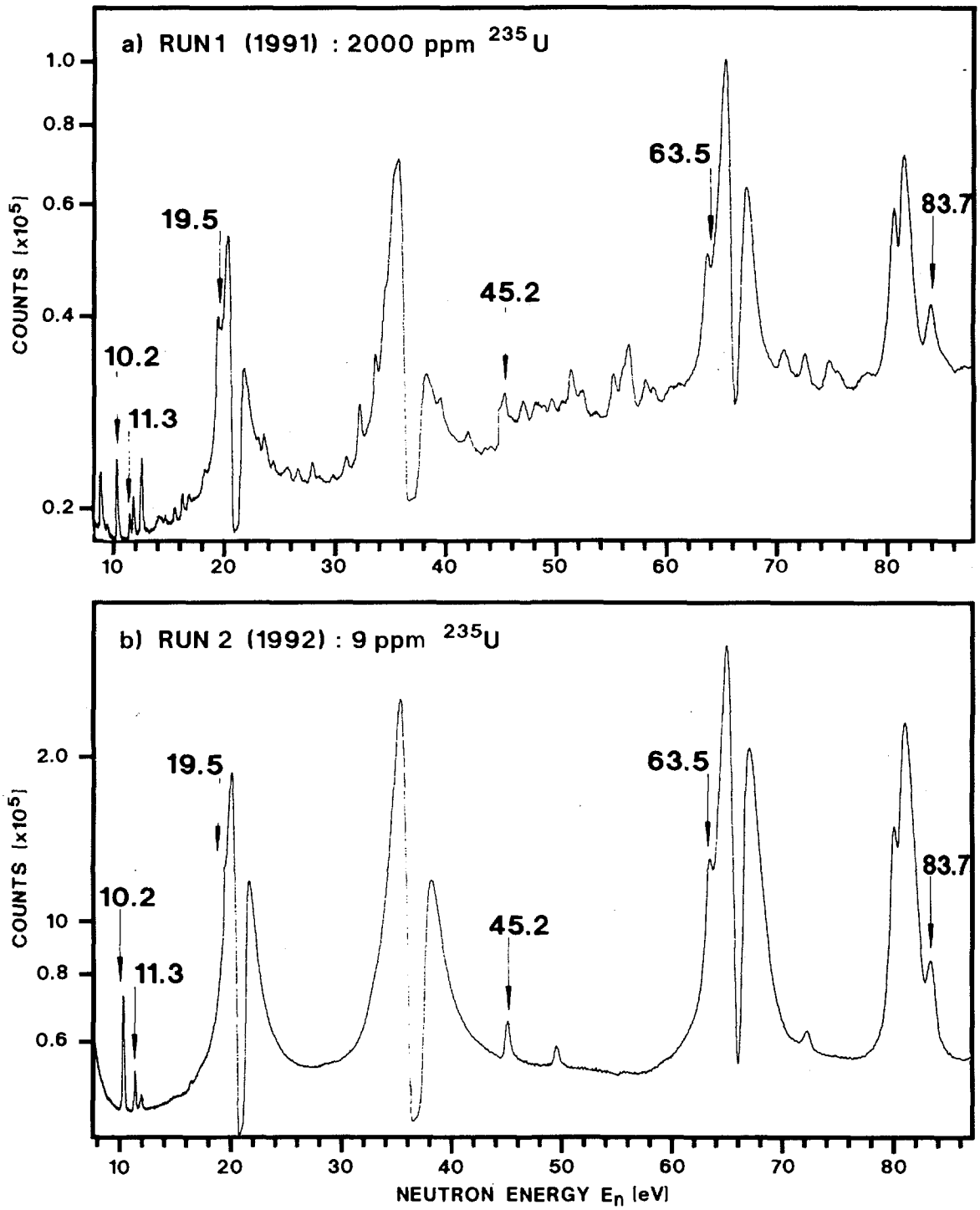

Fig. 19. Time-of-flight capture spectra as a function of the neutron energy: a) RUN 1 (1991), b) RUN 2 (1992)

The measurement is continuing in order to reduce the statistical errors and to extend the assignment to weaker resonances.

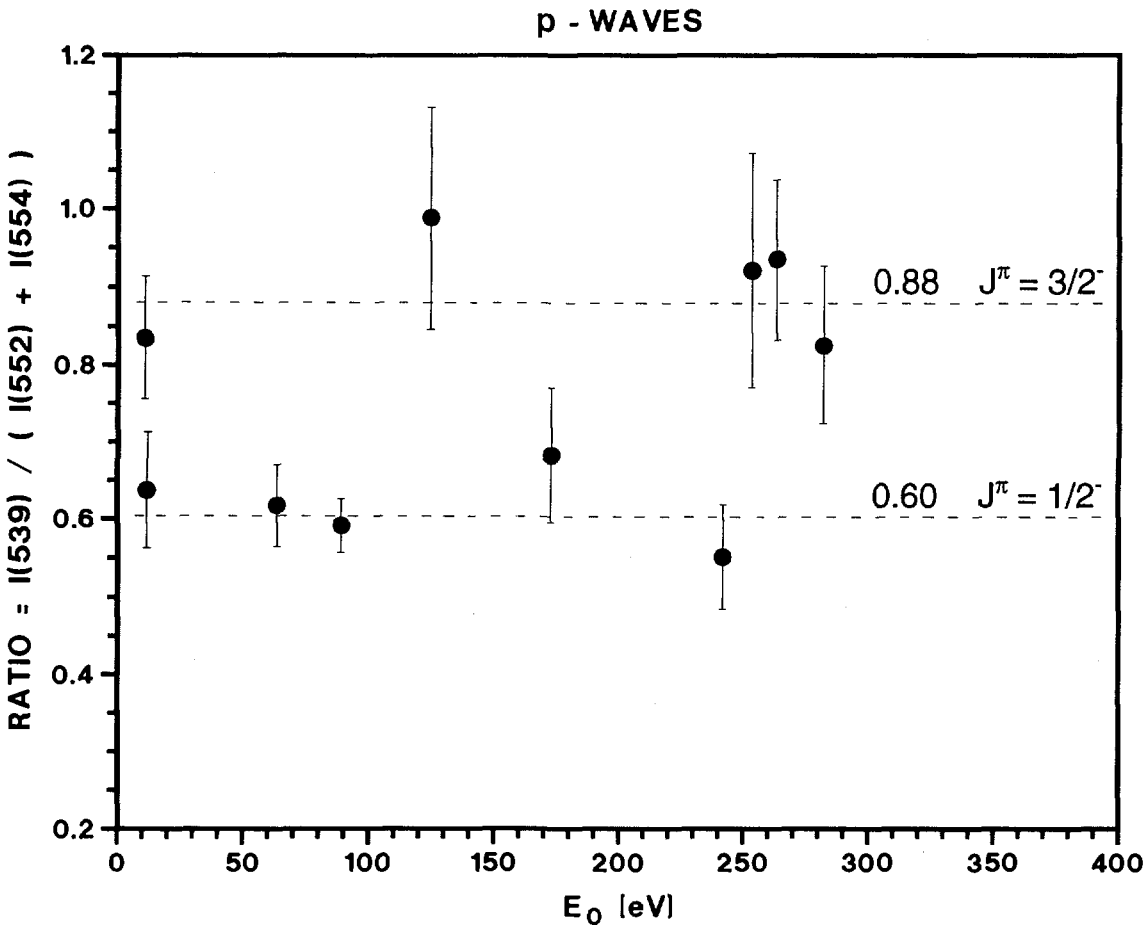

Fig. 20. Spin ratio as a function of resonance energy

Table 5. Results of the present spin assignment and values of the longitudinal asymmetry P for eleven ^{238}U p-waves

E_0 [eV]	Level spin J^{π}		$P = (\sigma_+ - \sigma_-)/(\sigma_+ + \sigma_-)$ [10^3]
	low-level popul.	primary trans.	
10.2	3/2	3/2	− 1.7 ± 0.9
11.3	1/2		7.2 ± 4.0
63.5	1/2		25 ± 4
89.2	1/2		− 2.4 ± 1.1
125.0	3/2		11 ± 9
173.2	1/2		11 ± 8
242.7	1/2		− 6.1 ± 6.2
253.9	3/2	3/2	− 1.6 ± 6.4
263.9	3/2	3/2	− 0.1 ± 4.1
282.5	3/2	3/2	3.8 ± 13
351.9		3/2	

Non-Statistical Effects Observed in s-Wave Neutron Resonances of ^{238}U

G. Rohr, R. Shelley

A very interesting non-statistical effect of the level spacings is observed in the s-wave neutron resonances of ^{238}U. This effect can be deduced from the sixteen spacings up to 380 eV as a function of the spacing sequence (number) observed with increasing neutron energy. The first two spacings are equal, the third is double and the fourth is once more the same spacing as for the first two. The first seven spacings are part of a regular spectrum with three different average spacings different by a multiple of 7.3 eV. The uncertainty of all average spacings is (7.3 × 0.15) eV. With increasing energy, distortions in the resonance spectrum can be observed for the spacing numbers 8, 9, 10 and 13. However, the sum of spacings 8 and 9 as well as 10 and 13 have a multiple of 7.3 eV and may give a hint to the reaction process.

The statistical relevance of the regular spacings can be discussed using a Wigner distribution with an average spacing of 20.2 eV calculated from the sixteen spacings. The probability to observe regular spacings at the energies of (M × 7.3) eV in the energy window (7.3 × 0.15) eV for randomly distributed values can be estimated. The results for M = 2, 3 and 4 are PM = 0.082, 0.073 and 0.048, respectively. According to this the detection of two consecutive spacings with M = 2 for a random sample is $0.67 \cdot 10^{-2}$. The probability for the first seven spacings being regular is less than $2 \cdot 10^{-8}$, and is statistically excluded. Therefore the observation of only three successive regular spacings in the energy windows of ± 15 % are relevant for a non-statistical effect.

The nearest level spacing distribution for resonances below 380 eV contains four peaks. In contrast the level distribution of simple resonances for nuclides A < 100 (^{40}Ca, ^{54}Fe, ^{58}Fe and ^{96}Zr) has less structure and could be called a Gaussian-like distribution. With the inclusion of ^{238}U resonances up to 2000 eV the level distribution approaches a Wigner function. Therefore the nearest level spacing distribution for simple resonances and medium light nuclides changes from a Gaussian-like function to a distribution containing several peaks for medium heavy and heavy nuclides. When resonances of higher energy are included the distribution approaches a Wigner function.

γ-Ray Decay Towards the Isomeric Groundstate in ^{239}U

S. Oberstedt*, F. Gunsing**, F. Corvi

The 721.6 eV-resonance in $^{238}U + n$ is assumed to be a nearly pure class-II state. Therefore its capture γ-ray spectrum should show lines corresponding to the

* EC Fellow from Technische Hochschule Darmstadt, Germany
** EC Fellow from Technische Universiteit Delft, The Netherlands

decay within the second potential well. In a high resolution measurement of γ-rays from neutron capture in ^{238}U four hitherto unknown γ-ray transitions could be found in the 721.6 eV-resonance as indicated in the upper part of Fig. 21. They are not observed in any other ^{238}U resonance. For comparison the γ-ray spectrum of the 661.14 eV resonance, which is a pure class-I state, is shown in the lower part of Fig. 21. This first indication for γ-ray transitions towards the isomeric state has to be validated by a more quantitative analysis.

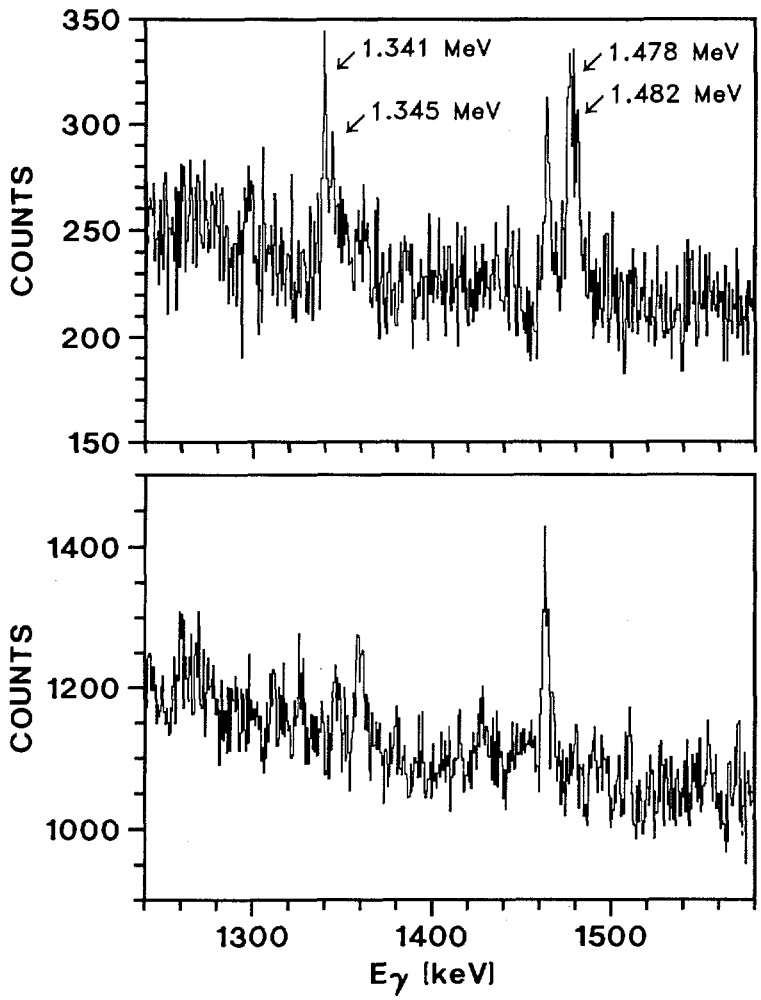

Fig. 21. *γ-ray energy spectrum of the 721.6 eV-resonance (upper part) with the four transitions indicated. The lower part shows the γ-ray spectrum of the 661.14 eV-resonance for comparison*

Resolution Function of Neutron Time-of-flight Measurements

C. Coceva*, M. Magnani**

In neutron cross-section measurements performed at the time-of-flight GELINA facility, a precise knowledge of the resolution function is of essential importance for the deduction of reliable values of resonance parameters, as required in various nuclear applications.

This resolution function results from the convolution of three independent components:

1) Time distribution of fast neutrons generated within the Linac target.
2) Delay time distribution, from the generation of neutrons to their escape from the target-moderator assembly.
3) Delay time distribution, from neutron entrance into the detector material to the corresponding detection time signal.

Part 1) follows closely the time distribution of the accelerated electrons as they impinge on the target.

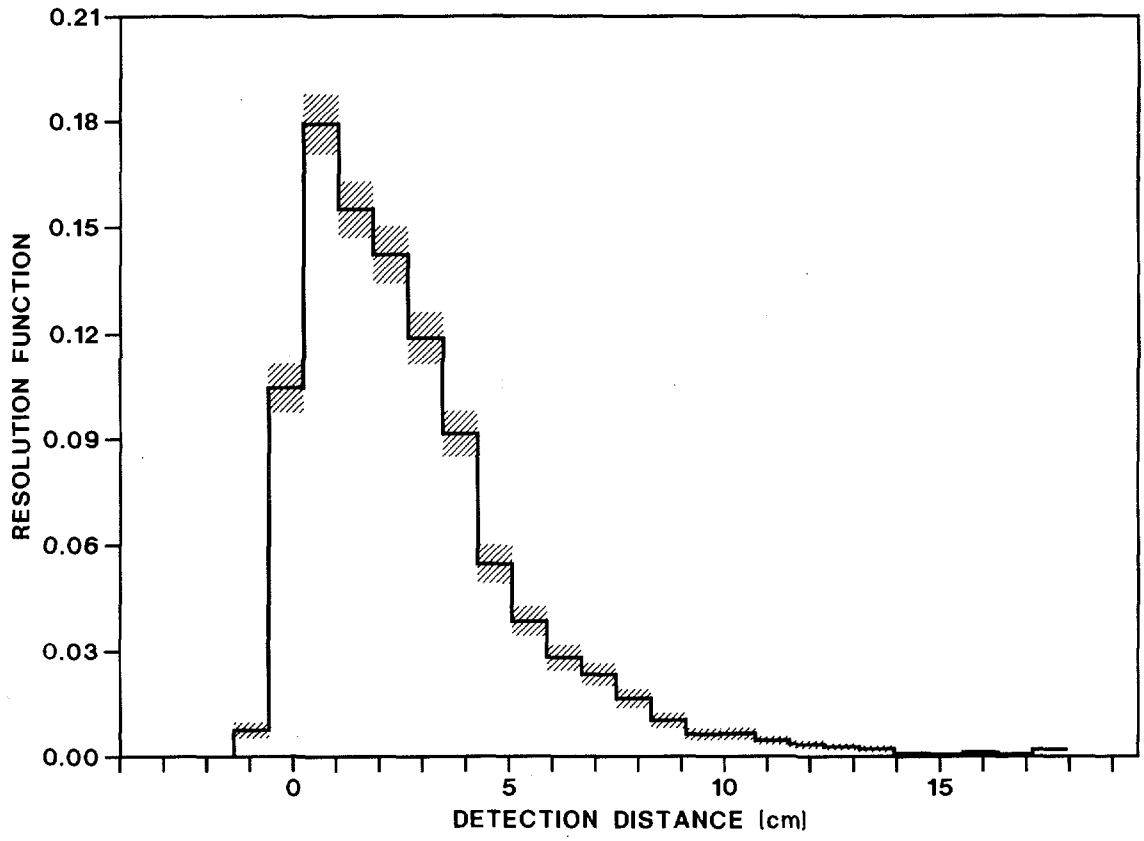

Fig. 22. Calculated resolution function for neutrons escaping from the moderator at 0° and with final energies in the range from 50 up to 250 keV

* Visiting Scientist from ENEA, Bologna, Italy
** ENEA, Bologna, Italy

For the contribution 2) a Monte Carlo simulation was performed considering the spacial distribution of the neutron source, the rotating uranium target, the cooling system, and the water-beryllium moderator tanks[1, 2]. Neutron distributions were obtained for energies from 4 eV to 6 MeV and for each flight-path direction.

It was found that the large amount of material necessarily introduced by the geometry of the rotating target, produces long tails in the time distribution of the emitted neutrons, spoiling the resolution.

Fig. 22 shows a calculated resolution function for neutrons escaping from the actual rotary target-moderator assembly of GELINA.

Contribution 3) was obtained for two different detectors:

a) A ^{6}Li-loaded glass scintillator, in the neutron energy range of 30 eV - 300 keV;

b) A ^{10}B plug, in the neutron energy range of 100 eV - 200 keV.

The above calculations were performed by means of a Monte Carlo simulation too[3]. In all cases, JEF cross-section data files were employed.

High Resolution ^{138}Ba (n,γ) Measurements

F. Corvi, H. Beer*, A. Mauri**, K. Athanasopoulos

The overall structure of s-process nucleosynthesis is determined by a few small capture cross sections of isotopes which form so-called bottle-necks for the s-process flow. One of the most important nuclides is ^{138}Ba , with magic neutron number 82, which is half way between the iron seed (A = 56) and the s-process termination at ^{209}Bi. The necessary strength of neutron exposure to build up the elements beyond mass number 142 is chiefly dependent on the size of the ^{138}Ba capture cross section. For a test of the current stellar double pulse s-process model[4] (where neutrons are produced by the combined burning of the ^{13}C(α,n) and ^{22}Ne(α,n) reactions at temperatures of kT = 12 and 25 keV, respectively) a precise ^{138}Ba stellar reaction rate as a function of kT is needed. This requires the knowledge of the ^{138}Ba(n,γ) excitation function from a few eV to about 200 eV.

High resolution neutron capture measurements were performed at a 28.4 m flight path using a $BaCO_3$ sample of 43 g, enriched to 99.8 % ^{138}Ba. A total of 54 neutron resonances were resolved and analysed in the energy range 0.2 - 105 keV in order to derive their capture areas. In particular two strong resonances

---

* Visiting Scientist from KFK, Karlsruhe
** National Expert from ENEA, Bologna

(1) A. Bignami, C. Coceva and R. Simonini, EUR 5151e (1974)
(2) C. Coceva, R. Simonini and D.K. Olsen, Nucl. Instr. Meth. 211 (1983) 459
(3) C. Coceva, P. Giacobbe and M. Magnani, Nucl. Sci. Eng. 91 (1985) 209
(4) R. Gallino, in Evolution of Peculiar Red Giant Stars, eds. H. R. Johnson, B. Zuckermann, Cambridge University Press, 1989, p. 176

at E_0 = 0.648 and 1.946 keV were observed for the first time. The data were normalized to capture in gold at 4.9 eV employing the saturated resonance method. The Maxwellian-averaged capture cross section $<\sigma_\gamma v>/v_T$ calculated from the present data is given as a function of kT in Table 6 and compared in Fig. 23 to a curve from ORNL and to an activation data point at 25 keV from KFK.

Table 6. Maxwellian-averaged (n,γ) cross section of ^{138}Ba for various kT values

kT [keV]	$<\sigma_\gamma v>/v_T$ [mb]	kT [keV]	$<\sigma_\gamma v>/v_T$ [mb]
10	7.64 ± 0.52	25	4.38 ± 0.34
12.5	6.53 ± 0.46	30	4.02 ± 0.30
15	5.79 ± 0.42	35	3.76 ± 0.35
17.5	5.27 ± 0.39	40	3.55 ± 0.38
20	4.90 ± 0.35	45	3.37 ± 0.40
22.5	4.61 ± 0.34	50	3.20 ± 0.43

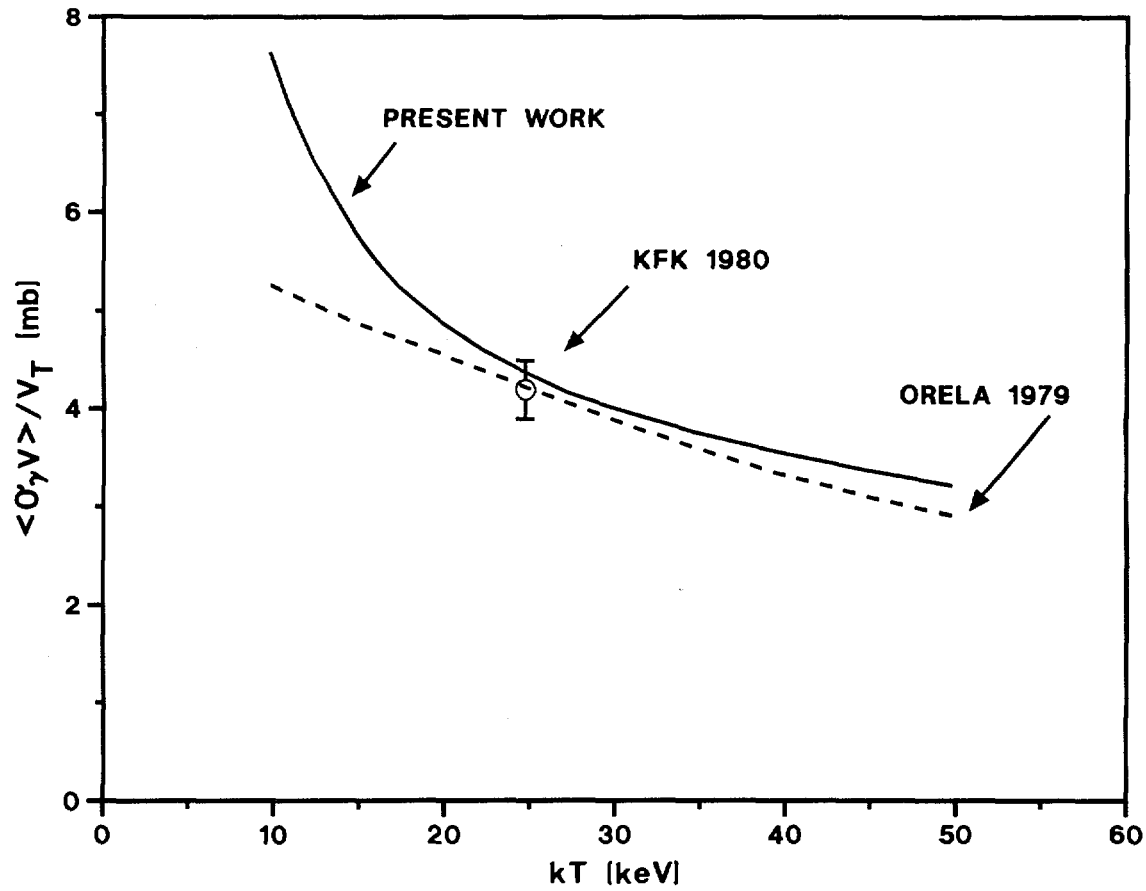

Fig. 23. The Maxwellian-averaged capture cross section vs stellar temperature

While both curves are compatible with the KFK value, their behaviour vs temperature is quite different. The present data suggest a much steeper rise with decreasing kT. This means that an s-process dominated by the burning of $^{13}C(\alpha, n)$ at kT = 12 keV can drive the synthesis through the bottle-neck ^{138}Ba up to lead and bismuth more efficiently also with a reduced neutron flux (~ 30 %) than according to the previous ORNL data. A much larger capture cross section at kT = 12 keV has also consequences for the ^{138}Ba s-process abundance if formed at this stellar temperature. This may concern the interpretation of the s-process nucleosynthesis in barium stars and s-process related isotopic anomalies of barium in meteorites.

^{4}He Emission in the Interactions of Fast Neutrons with ^{48}Ti and ^{50}Ti

S.M. Qaim*, M. Uhl**, N.I. Molla*, H. Liskien

Excitation functions were measured radiochemically for the $^{48}Ti(n,\alpha)^{45}Ca$ and $^{50}Ti(n,\alpha)^{47}Ca$ reactions over the neutron energy range of 12.6 to 19.6 MeV. Use was made of low-level anticoincidence β^-counting in the radioactivity measurement of ^{45}Ca and of high-resolution γ-ray spectroscopy in the case of ^{47}Ca. Statistical model calculations taking into account preequilibrium effects described the proton emission well; the calculated ^4He emission results were, however, consistently lower than the experimental data, both as regards emission spectrum and excitation function. Inclusion of a direct three-nucleon pickup component in the ^4He emission calculation improved the agreement between theory and experiment.

* Institut für Nuklearchemie, Forschungszentrum Jülich, Germany
** Institut für Radiumforschung und Kernphysik, Universität Wien, Austria

NUCLEAR METROLOGY

RADIONUCLIDE METROLOGY

The objective of the work on radionuclide metrology is to advance the experimental know-how in the field of radioactivity. This is done in four major areas: the determination of decay-scheme data, the improvement and development of measurement techniques, the preparation of particular standard and reference samples and the participation in international comparisons and evaluations.

Low-Energy X-Ray Standard Sources

B. Denecke, G. Grosse

Four sources of 5 MBq ^{55}Fe in the form of stable metallic layers were produced by electrodeposition onto small copper rings. The yield of electrolytic deposition was up to 60 %. A transport container with special tools for safe and precise positioning of the interchangeable fluorescence targets with respect to the excitation source was designed to hold up to ten fluorescence layers and the X-ray excitation source.

Measurement of K-Shell Fluorescence Yields

V.A. Solé*, B. Denecke, G. Grosse, W. Bambynek

There are only few measurements of the K-shell fluorescence yield of calcium reported in the literature. The results show a large scatter and disagree with predicted values. For potassium no measured data are reported. New measurements were made using metallic samples of calcium and potassium. In these layers K-shell vacancies were produced by photo effect using a collimated beam of manganese KX-rays, the emission rate of which was measured with a gas-flow proportional counter. The fluorescent radiation was measured with a windowless Si(Li) spectrometer at a defined low solid angle. Taking advantage of the standardized low energy X-ray sources developed by CBNM, the detector efficiency could be measured with an accuracy of about 1 %. The K-shell fluorescence yields are $\omega_K(Ca) = 0.164 \pm 0.004$ and $\omega_K(K) = 0.144 \pm 0.004$.

---

* EC Fellow from the University of Valencia, Spain

Standardization of α-Particle Emitting Samples

B. Denecke

A cooperation with NIST was started to measure with highest achievable accuracy the emission rate of α-particle emitting samples prepared at CBNM. Three ^{233}U samples have been measured at two different defined low solid angles. They will be measured independently also at NIST. The data evaluation is in progress.

Second EUROMET Intercomparison of ^{192}Ir Brachytherapy Sources

D.F.G. Reher

The evaluation of the results from the second EUROMET intercomparison of ^{192}Ir brachytherapy sources showed that there were problems for the mass determination of the highly radioactive wires, the calibration of ionization chambers in terms of activity, and the interpretation of calorimeter measurements. In most cases the sources of error could be identified and improvement was achieved. The results of this second intercomparison will be published in 1993.

Standardization of a ^{152}Eu Solution

D.F.G. Reher, T. Altzitzoglou, B. Denecke, E. De Roost

For the standardization of a 50 GBq $^{152,154}Eu$ volume source used to determine the linear power dissipation of irradiated fuel pins from material testing reactors, it was necessary to standardize a ^{152}Eu solution. A 2 ml mother-solution with an activity concentration of 100 MBq/g having a ^{154}Eu impurity of 1.32 % was prepared from material obtained from Amersham. From this solution 5 dilutions, 17 quantitative solid sources and 3 solutions in standard ampoules were prepared. For the standardization two independent methods were chosen: the $4\pi\beta$-γ-coincidence method and 4π-CsI spectrometry. The complexity of the ^{152}Eu decay scheme was of advantage for the measurements with the 4π-CsI sandwich spectrometer (redundant radiation cascades), whereas the actual set-up of our $4\pi\beta$-γ-coincidence system produced results which depended strongly on the cut-off energy in the γ-channel. An example of a spectrum obtained with the 4π-CsI spectrometer is shown in Fig. 24. The only significant correction applied was the low energy cut-off correction of about 0.4 %. The solution was standardized with an uncertainty of 0.4 % (one standard deviation).

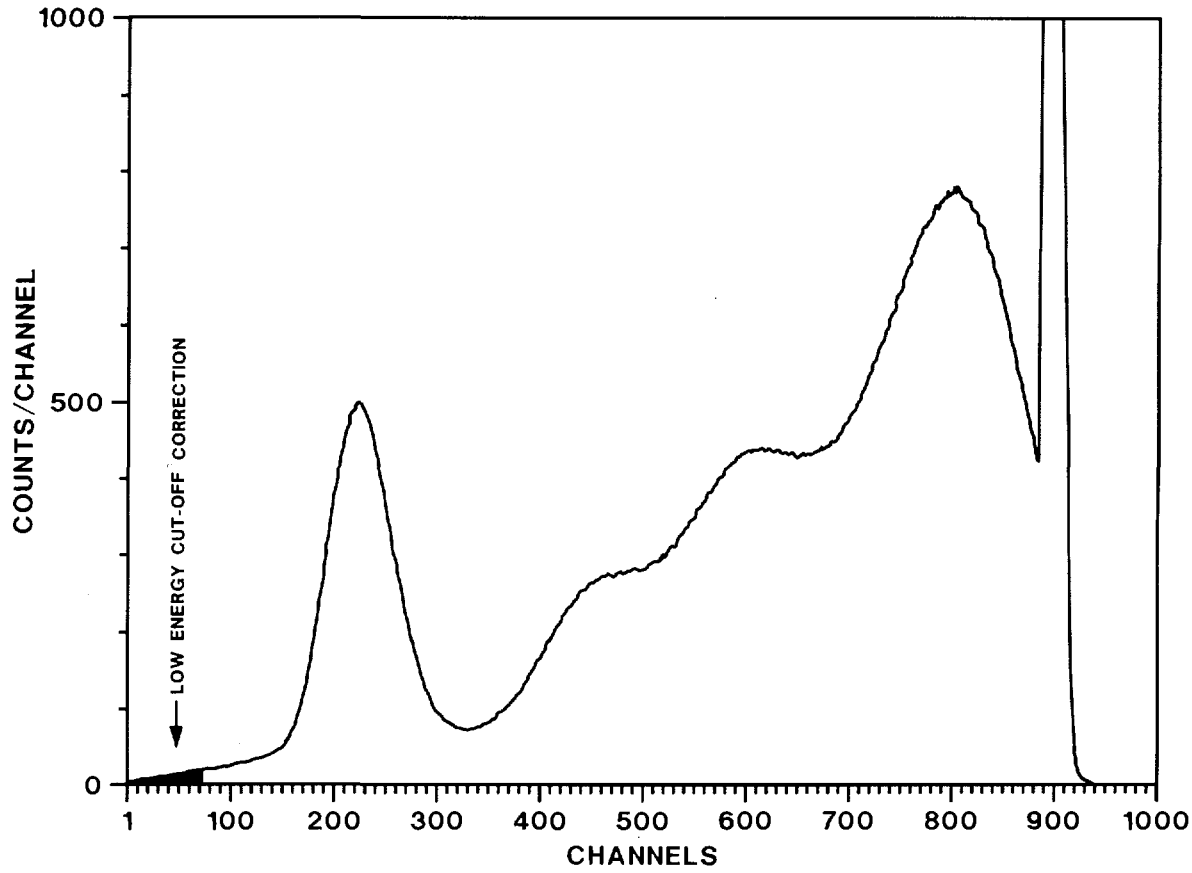

Fig. 24. A typical spectrum of ^{152}Eu obtained with the 4π-CsI spectrometer

Efficiency Curve for the CBNM Radionuclide Calibrator

D.F.G. Reher, G. Sibbens

The CBNM radionuclide calibrator is a well-type ionization chamber (20th Century Electronics, type IG-12) which has been calibrated for various radionuclide solutions in NIST/BIPM standard ampoules. Calibration always requires highly pure standards. However, often secondary standardization of material with significant impurities has to be done. Furthermore, one needs to standardize a radionuclide solution for which no calibration figure is available. In these cases an efficiency curve as a function of energy is needed. Such a curve was established (Fig. 25) using preferably nuclides emitting only a single γ-ray. Additionally, we could use data points measured by Urquhart[1] with the same type of ionization chamber.

(1) D.F. Urquhart, Calibration and Operation of the AAEC Working Standard of Measurement for the Activity of Radionuclides, AAEC Report 1986

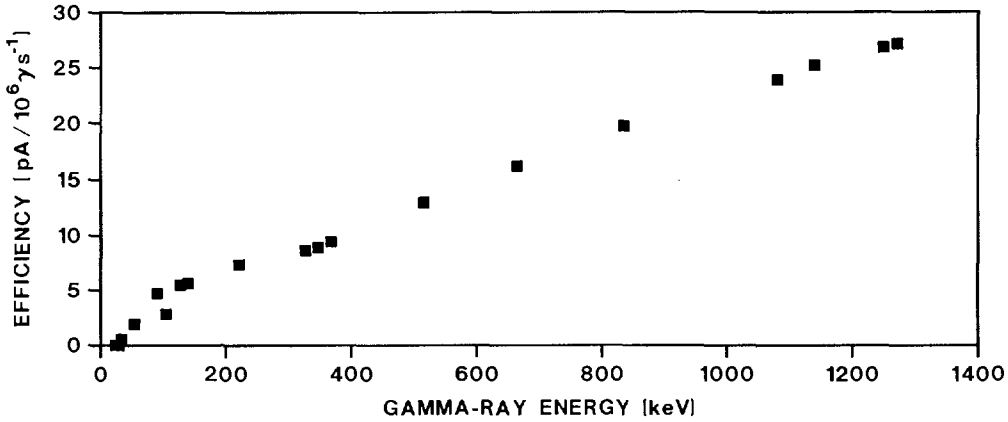

Fig. 25. The CBNM radionuclide calibrator efficiency curve

Investigation of the Natural Radioactivity in Volcanic Rock Samples Using a Low Background γ-Ray Spectrometer

R. Wordel, D. Mouchel, V.A. Solé*

A low-level HP Ge detector system was used to investigate powdered volcanic rock samples of different origin. An efficiency calibration of the detection system was performed with a powdered solid source, spiked with suitable radionuclides and having a chemical composition close to that of the investigated samples. To obtain the full-energy-peak efficiency ε_γ for the different extended samples corrections for geometry, self-absorption and absorption have been applied using a Monte Carlo programme.

The studied samples originate from the Eastern Sunda Volcanic Arc in Eastern Indonesia, where the subduction of the Australian plate under the Asian plate takes place. The samples were taken from volcanoes, at places where the depth of the Australian plate varies from 100 to 300 km. The concentration of radionuclides from the natural decay chains in the samples was compared with that in a well known reference sample. A correlation between some of the radionuclide concentrations and the subducting depth was established.

Measurement of Low-Level Radioactivity in Archaeological Ceramics

R. Wordel, D. Mouchel

On request and in collaboration with the Technical University of Munich (D), measurements of low-level radioactivity in archaeological ceramics of Celtic origin, using a low-level HP Ge γ-ray detection system were done. The place where the samples were excavated is situated close to Manching (D). The aim of the measurements was to characterize the clay on the basis of natural

* EC Fellow from the University of Valencia, Spain

radionuclides and to study a possible disequilibrium in the natural decay series for a geological identification of the clay used to produce the Celtic pottery.

Measurement of Low-Level Radioactivity in soil and river sediment
R. Wordel, D. Mouchel

Determination of radionuclide concentrations in soil, sand and aquatic samples collected close to an industrial site, and also from unpolluted areas has been performed. Field samplings, sample preparation (17 samples) and measurements in Marinelli beaker geometry were done. The data analysis is in progress. Fig. 26 shows two strongly varying spectra of river sediment samples together with a background measurement. Both, the total radioactivity and the ratios between different natural radionuclides are very different.

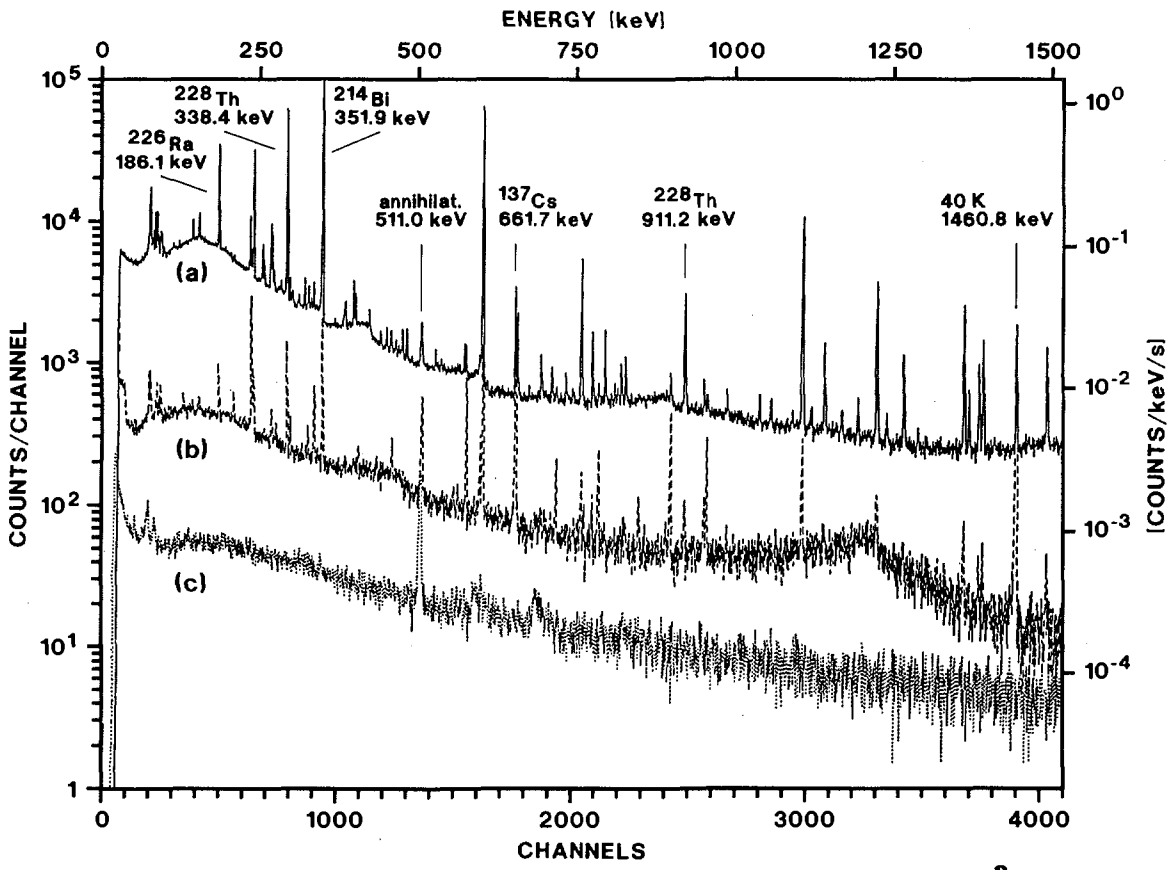

Fig. 26. ***Spectra recorded during two days with a low-level 100 cm^3 intrinsic Ge detector: (a) river sediment samples close to the industrial facility and (b) similar samples collected far from any industrial site. (c) background***

Further Reduction of Background
R. Wordel, D. Mouchel

In collaboration with SCK/CEN, Mol (B), in the underground laboratory HADES a study is going on to reduce the background of a low-level high-purity

Ge detection system. First results with the shielded system show an integrated count rate within the energy interval (70 - 3000) keV of (0.0156 ± 0.0006) s^{-1}. The reduction with respect to the same detector and shielding situation in the counting room at sea level is larger by a factor of 30, and by about 3200 if one compares with the unshielded system at sea level.
The achieved sensitivity for γ-ray spectroscopy reaches below mBq/kg corresponding to better than 10^{-10} g/g of uranium and thorium.

Modelling of Alpha-Peak Shape

E. Steinbauer*, P. Bauer*, J.P. Biersack**, G. Bortels

The work dealt with the influence of plural and multiple scattering of high energy projectiles in two characteristic applications: Rutherford backscattering spectroscopy (RBS) and the response of particle implanted and passivated silicon detectors (PIPS) to monoenergetic MeV alpha particles.
The detector response to 3183 keV alpha particles is calculated using a detector model, which assumes a dead layer near the front contact followed by a fully sensitive volume. All model parameters are determined either from theory or from measurements. The calculated alpha spectrum perfectly agrees with the measurement both in the resolution (FWHM) and in the asymmetric shape.

Alpha Spectrometry in Relation with Calorimetry

G. Bortels

Most important transuranics are alpha-particle emitters. More than 99 % of their heat output is due to alpha emission and the associated recoil energy. Therefore, alpha spectrometry is a complementary measurement technique to the non-destructive calorimetric measurements. Current achievements with alpha spectrometry at CBNM, in particular with respect to the measurement of $^{239}Pu/^{240}Pu$ and $^{238}Pu/^{241}Am$ mixtures were described in a conference paper.

Installation of a New Liquid Scintillation Counter (LSC)

T. Altzitzoglou

A commercial LSC has been installed for the standardization of β-particle emitters of interest in various fields e.g. metrology, nuclear medicine

* Institut für Experimentelle Physik, Universität Linz, Austria
** Hahn-Meitner Institut Berlin, Germany

diagnostics and environmental studies. It includes the feature of pulse shape discrimination to distinguish pulses produced by alpha or beta particles.
The time resolving circuitry allows, in connection with the new generation of liquid scintillation cocktails, to significantly reduce the background.
The computer programme EFFY4[(1)] has been implemented in a personal computer. It calculates the theoretical counting efficiency for a given nuclide and links that to the figure of merit and the quench factor given by the instrument. Then, a single quench curve (normally obtained using tritium samples) is sufficient to calculate the quench-corrected efficiency for any β-particle emitting nuclide that is measured.

TDPAD STUDIES AT THE 7 MV VAN DE GRAAFF

The technique of time-differential perturbed angular distributions (TDPAD) of γ-rays has been used with the pulsed beam facility at the Van de Graaff for the study of pure and applied physics issues in some selected cases.

Search for the Quadrupole Moment of the 583 keV State in ^{22}Na

F.-J. Hambsch, P. Martin*, H. Postma**, P. Rietveld, D. Surono***

An experimental determination of the quadrupole moment of the 583 keV ($J^{\pi} = 1^+, T_{1/2} = 243$ ns) level in ^{22}Na provides a basis for differentiating between the deformed or shell model descriptions of the nucleus. On a pure shell model basis, a half-filled shell of $d_{5/2}$ protons and neutrons should produce a zero quadrupole moment for this state. On the other hand, rotational models or shell models with mixed configurations indicate that $Q \sim 0.06$ b. Highly oriented pyrolytic graphite (HOPG) was used as a substrate for recoil implantation of ^{22}Na produced by the $^{19}F(\alpha,n)^{22}Na$ reaction. The large electric field gradient expected in HOPG ($\sim 10^{18}$V/cm^2) can interact with the quadrupole moment of the ^{22}Na state to produce a perturbation of the γ-ray angular distribution, such as that shown in Fig. 27 for the 197 keV state ($J^{\pi} = 5/2^+$, $T_{1/2} = 89$ ns) of ^{19}F. In the case of ^{22}Na, however, no perturbation is observed for the 583 keV level, as evidenced by the flat spectrum shown in Fig. 28. Results indicate that $Q < 0.005$ b for the ^{22}Na state, and are consistent with a pure $d_{5/2}$ shell model description.

---

* Visiting Scientist from the University of British Columbia, Vancouver, Canada
** Visiting Scientist from Technical University of Delft, The Netherlands
*** PhD Student from the University of British Columbia, Vancouver, Canada
(1) Garcia-Toraño, E. and Grau, A. "EFFY, a New Program to Compute The Counting Efficiency of Beta Particles in Liquid Scintillators", Comp. Phys. Comm. 36 (1985) 307

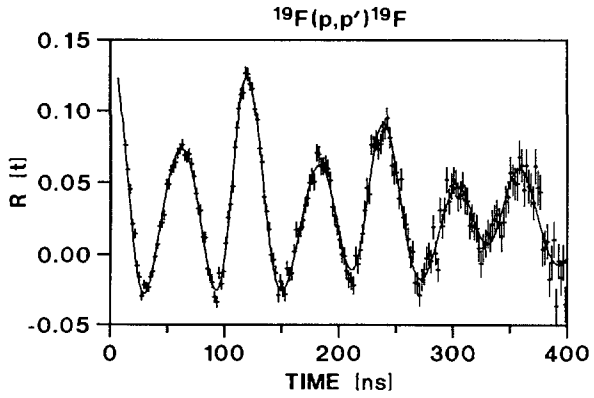

Fig. 27. Perturbation spectrum for the 197 keV level of ^{19}F in HOPG

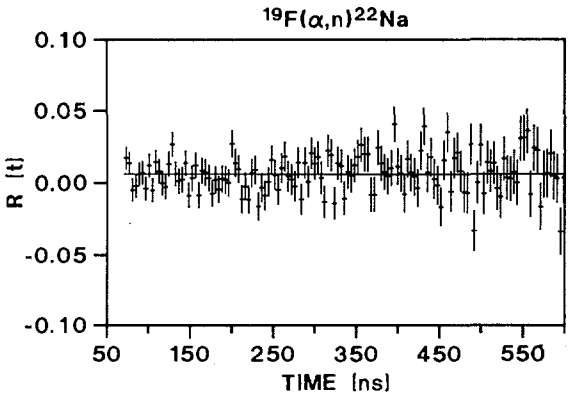

Fig. 28. Perturbation spectrum for the 583 keV level of ^{22}Na in HOPG

Fluorine Residence Sites in Silicon and Germanium

F.-J. Hambsch, P. Martin*, P. Rietveld, D. Surono**

The role of fluorine in the manufacture of semiconductors is extremely important; it can control key parameters such as doping efficiency, improve photovoltaic characteristics, reduce leakage currents in p-n junctions and increase the reliability of metal oxide semiconductor (MOS) capacitors. Using the $^{19}F(p,p')^{19}F$ reaction, fluorine was recoil implanted from thin films of CaF_2 into silicon and germanium substrates. The interaction of the quadrupole moment of the 197 keV state of ^{19}F with the local electric field gradient within the substrate material was used to determine the nature of the residence sites. An example of the results together with theoretical fits are shown in Figs. 29 and 30 for silicon (111) and germanium (111) samples respectively. The industrial heat treatment of fluorine-doped silicon and germanium is a major factor in affecting the role played by fluorine in these materials.

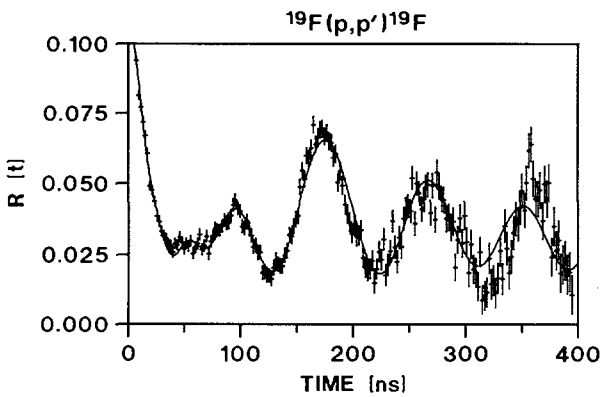

Fig. 29. Perturbation spectrum for the 197 keV level of ^{19}F in silicon

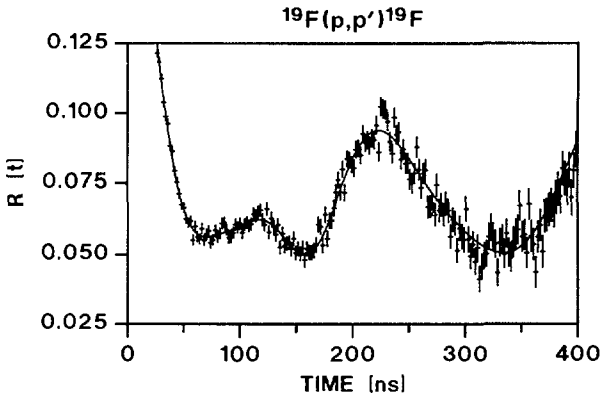

Fig. 30. Perturbation spectrum for the 197 keV level of ^{19}F in germanium

* Visiting Scientist from the University of British Columbia, Vancouver, Canada
** Ph-D Student from the University of British Columbia, Vancouver, Canada

Further studies will be pursued to investigate the residence sites in previously fluorine-implanted samples subjected to different heat treatment protocols. Identification of the fluorine sites should then help to elucidate the role played by the fluorine in altering the physical behaviour of MOS devices.

Radiation Damage Studies in GaAs

F.-J. Hambsch, P. Martin*, D. Surono**

Using the $^{71}Ga(p,n)^{71}Ge$ reaction on a GaAs target, a flat perturbation spectrum was obtained for the 175 keV ($J^{\pi} = 5/2^{+}$, $T_{1/2} = 84$ ns) level of ^{71}Ge. Since GaAs has cubic symmetry and consequently zero electric field gradient, the result implies that the ^{71}Ge also experiences a cubic environment. Consequently TDPAD will be used to investigate the effects of impurities and radiation damage in GaAs.

---

* Visiting Scientist from the University of British Columbia, Vancouver, Canada

** Ph-D Student from the University of British Columbia, Vancouver, Canada

TECHNICAL APPENDIX

Electron Linear Accelerator

J.M. Salomé

The GELINA electron beam was available during 2325 hours for physics experiments.

Neutrons are produced in a rotary uranium target via (γ,n) and (γ,f) reactions. According to the requested neutron energies, various moderators are placed on both sides of the target. Twelve flight paths are equipped for neutron time-of-flight experiments. On the average, 5.7 neutron beams were used simultaneously when GELINA was operated at very short bursts and 3.3 of them when operated in other conditions.

On the main electron beam line of 0°, an optical transition radiation system (10 μ aluminium radiator foil) is used to determine some parameters of the beam as divergence and energy. However, the divergence growth due to the radiator foil perturbs the operation of the compression magnet. Thus, such measurements will be made only to adjust the electron beam and the radiator will be removed in normal operation.

To one side of the main line, a 40 MeV electron beam has been deflected to allow experiments with X-ray transition radiation. This set-up is suitable for measurements at very low currents with various radiators.

For radiation protection reasons the target room may be closed with lead doors when the neutron beams are not in use. In view of improving the staff protection, the control system of these doors was completely renewed.

The refurbishment of the Linac was started by placing the first orders at the end of the year. The work essentially will imply the replacement of the two long sections and the corresponding equipment in view of applications in neutron and radiation physics. The specifications are very stringent concerning the performance of the new parts which will have to be matched for the achievement of the low emittance electron beam needed for the radiation physics experiments. The modernised Linac should be ready by the end of 1994 after a six months period of breaking its operation.

The present experimental possibilities in the neutron target hall are not adequate for the radiation physics programme. Therefore, a new experimental hall is foreseen at the 0° beamline outside the target hall. The drawings for this new experimental hall have been completed and the order placed. Ground works will start in early 1993. A new system to extract the electron beam at 0° by remote control has been designed. It will allow to use the electron beam alternatively for the neutron physics or for the radiation physics programmes.

Radiation Physics

R. Cools, P. Goedtkindt*, O. Haeberlé**, N. Maene***, F. Poortmans***, H. Riemenschneider, P. Rullhusen, J.-M. Salomé, F. Van Reeth

X-ray Transition Radiation.

Transition radiation is a very promising technique for production of intense soft X-ray beams at energies of about 1 keV using electron accelerators[1]. One week of beam time was used to accomplish the final measurements of X-ray energy spectra and angular distributions for the thesis of P. Goedtkindt. The data have been evaluated and the thesis is nearly completed.

At the end of this measuring period also a multilayer, which was provided by the University Pierre et Marie Curie, Paris, has been used as radiator. This experiment was done in order to look for a new radiative effect proposed. No effect was seen, which could, however, be due to the rather bad beam quality.

Optical Transition Radiation.

The new techniques envisaged for the radiation physics programme at GELINA require an excellent beam quality, which will be available after the second step of the proposed refurbishing plan. A system has been installed to perform beam emittance measurements using optical transition radiation. The system is running well and is able to deliver online information about the electron energy, the beam size and the beam divergence. An internal report has been prepared[2].

Smith-Purcell effect.

The Smith-Purcell effect is attracting considerable interest in several laboratories (i.e. Mainz, Darmstadt, Brookhaven, Lawrence Livermore, Oxford). The idea is to use this effect to produce intense X-ray beams using ultrarelativistic electrons travelling close to a metallic grating. Unfortunately, no rigorous theoretical treatment has been published yet and only one experiment has been achieved in the far infrared using a rather moderate electron energy of 3.6 MeV. A new mathematical algorithm has been developed on the basis of the Greens-function method proposed for optical diffraction in order to calculate the Smith-Purcell radiation emitted by ultrarelativistic electron beams. The code works well for rectangular and sinusoidal gratings and is being extended to apply also to more general gratings. An experiment at optical wavelengths using a 100 MeV electron beam at GELINA is envisaged.

---

* EC Fellow. Present address: Université Paris Sud, LSAI, Orsay, France
** EC fellow from Université de Strasbourg, France
*** VITO, Mol, Belgium
(1) CBNM Annual Report 91, EUR 14374 EN
(2) S. Schaeffer, Internal Report GE/R/LI/1

Measured Fast Neutron and Gamma-Ray Fluence Close to the GELINA Target

W. Schubert, C. Tsabaris*, E. Wattecamps

In preparation to perform radiation damage irradiations by fast neutrons at a fluence level of 10^{15} n/cm^2 and larger within irradiation times of some hours or days, the fast neutron and γ-ray fluence at 46 cm distance from the GELINA target at various spots in a horizontal plane at 23 cm below the target have been measured. The machine was operated at 150 MeV electron energy and 6 kW beam power. The neutron energy spectrum and the neutron fluence were determined by the activation technique with a set of eleven threshold activation reactions.

An estimate of the gamma ray fluence was deduced from γ-ray activation measurements relying on the reaction $^{59}Co(\gamma,n)^{58}Co$.

Details of the experiment and a discussion of the results are given elsewhere[1,2].

The measurements lead to the following conclusions:

- the neutron yield is strongly angular dependent and the largest fluence was observed at a neutron emission angle around 115 degrees;
- at 6 kW beam power the neutron flux at 46 cm distance from the target, amounts to $7.4 \cdot 10^8$ n/s·cm^2, and the γ-ray fluence is at least $2.5 \cdot 10^8$ γ-rays/s·cm^2;
- assuming an isotropic neutron yield distribution a source strength of $1.96 \cdot 10^{13}$ n/s in 4π sr is deduced from the activation measurements.

Van de Graaff Accelerators

A. Crametz, P. Falque, J. Leonard, W. Schubert

The total working time of the two accelerators was 4677 hours. The experiments at the 7 MV were divided in 1107 hours for non-neutron activities (NRA and TDPAD) and 1314 hours for neutron activities (data for standards and for fission and fusion technologies).

The CN-7MV accelerator has been opened for the replacement of the RF ion source and for the installation of a fourth gas bottle (^{3}He) in the high voltage terminal. For the first time a $^3He^+$-ions beam has been achieved.

---

* EC Fellow from University of Athens, Greece

(1) C. Tsabaris, W. Schubert and E. Wattecamps, Internal Report GE/R/VG/73/92

(2) W. Schubert and E. Wattecamps, Internal Report GE/R/VG/72/92

CBNM Computer Network

C. Bernard, C. Cervini, H. Horstmann, C. Nazareth, C. Van den Broeck*, L. Van Rhee, P. Van Roy

The X.400 message handling system of CBNM has been extended to VAX/VMS computer systems by the installation of the DFN-EAN software. X.400 message handling is now available for the IBM/MVS, VAX/VMS and XEROX/Viewpoint environment.
A 3380 disk storage system has been installed for the main computer (IBM 4381) of the CBNM computer network. Most of the data volumes on the old 3375 disk storage system have been moved to the new units.
SYSTRAN, a fully automatic language translation system in use at CEC Luxembourg, has successfully been tested by means of the X.400 mail system.
A study for a workgroup network based on PCs and the existing Ethernet has been made. The network server will be able to support DOS, Windows, OS2/2, MAC and UNIX workstations.
An IBM RS/6000 computer running under AIX has been installed and customized. Client server tests with a PS/2 have been made. A connection to the public X.25 network has been established. Some APL applications have successfully been downloaded from the IBM 4381 system.
Plans have been made to replace the present CPU of the IBM 4381 computer system by a second-hand unit of double processing power in early 1993.
A set of interactive graphic facilities for the analysis of neutron data measured at GELINA has been developed.

MPA/TP, a Multiparametric Acquisition System with Transputers

C. Bastian, S. de Jonge, J. Gonzalez

Hardware modules containing 16 bit transputers can be used to monitor simultaneously up to 4 detector signals per module. A chain of up to 4 of these modules may produce a stream of multiparametric events involving up to 16 parameters of a nuclear reaction together with their coincidence pattern.
On-line analysis of the event stream is performed with 32 bit transputers on commercial boards hosted by a microVAX II. Complex schemes of on-line event analysis can be described in few lines of a dedicated configuration language and implemented on the transputer network.
Standard VMS command files are available to compile any scheme of event analysis to a load module for the 32 bit transputer, to test the load module nominally and to implement it as a full MPA system in combination with listing or histogramming facilities of the host. A user's guide is in preparation.

---

* COMPAREX, Brussels, Belgium

The AGS File System for Spectrum Analysis

C. Bastian

A new file format AGS (Analysis of Geel Spectra) was designed for the storage and the off-line analysis of multichannel counting spectra. All steps of an analysis can be saved in a single AGS file, starting from raw experimental results (counting histograms) and resulting in a series of cross section values. The results of the analysis are stored as integer or floating point spectra, including experimental constants, channels bounds, observation vector and covariance matrix.

In the AGS system, the analysis is performed in elementary steps (e.g. deadtime or background correction). Every step is a program reading results of the previous steps as spectra from the file and appending new results to the file. A basic set of AGS programs is already available in C. It may be complemented ad libitum by user-written programs, using a dedicated function library for e.g. spectral data access, matrix operations or covariance propagation.

Handling Large Data Amounts

F. Gunsing*, C. Nazareth, P. Ter Meer, C. Cervini

For the experiment of spin assignment of ^{238}U an amount of 300 Mbyte per measuring day with a total in the order of 10 Gbyte has been collected with a PC-based FAST Data acquisition system.

Originally the data were transferred each day from the PC hard disk via Ethernet to the IBM 4381 mainframe and there backed up onto tape and sorted into spectra.

The transfer rate was on average about 30 kbyte/s resulting in nearly three hours of transfer time a day. During this period, data acquisition on the FAST was halted whilst job running on the mainframe were processed very slowly because of conflicting priorities.

Data are now transferred to the Micro VaxII giving a transfer rate of 80 kbyte/s. Then the data are backed-up onto an Exabyte 8200 unit having a capacity of 2.5 Gbyte per data casette. The transfer does not significantly affect processes running on the Micro Vax.

On a Macintosh Quadra 700 system, a program has been developed to sort the data using the sorting algorithm of the mainframe. The data, which are stored on the Micro Vax, are fully transparent to the Macintosh via Ethernet due to special client/server network software. The spectra are then available for analysis programs used on the Macintosh. At the end of the experiment,

---

* EC Fellow from the Technical University of Delft, The Netherlands

accumulated data can be sent to the mainframe by one single file transfer where they are available in the IFSPEC format for use by other analysis programs.

LISA - LIstmode and Spectral Data Analysis

A. Oberstedt*, F.-J. Hambsch

LISA is a programme package which enables both off-line listmode and spectral data evaluation as well as on-line monitoring while multiparameter experiments are running. This program has been developed on and for SUN - workstations, but can be executed in principle on every computer under an UNIX operating system with an X-WINDOW environment and running PV-WAVE from Precision Visuals Inc. This package is basically written in the language PV-WAVE CL which provides a powerful treatment and a fast visualization of large multidimensional datasets. Integration of subroutines written in the C-language and execution of UNIX shell commands leads to an additional increase of performance.

Besides providing maximum speed, optimum comfort for users was aimed. This could be reached by standardizing all routines as far as possible. Going more

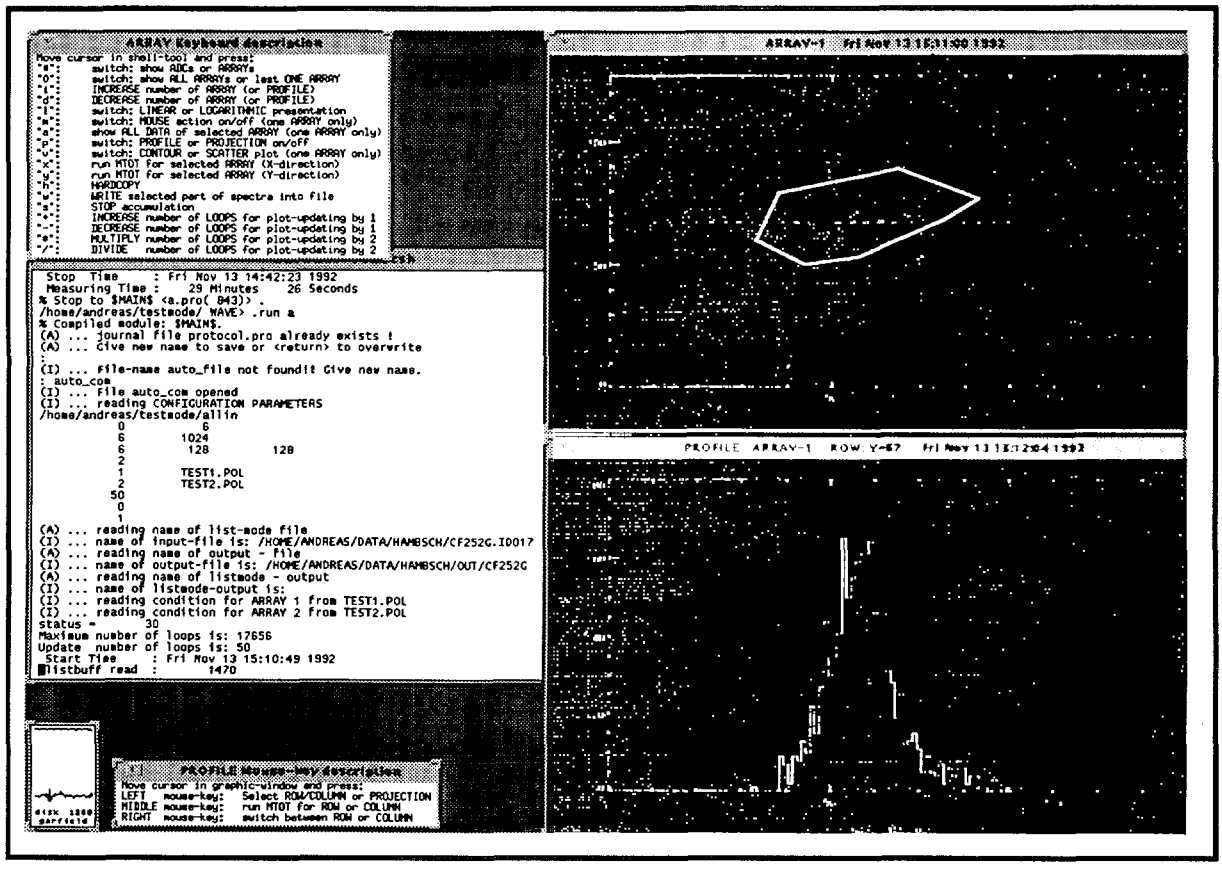

Fig. 31. ***Typical workspace for data evaluation with LISA. A two-dimensional configuration as well as a profile is displayed. Possible mouse and keyboard actions are shown***

* Visiting Scientist from Technische Hochschule Darmstadt, Germany

into details this means that users only have to input a few characteristic parameters either interactively or by the more convenient way using a command file to get an immediate visualization of their raw data. For data evaluation, concerning data modification, calculations or creation of new datasets, the user is obliged to write a small C-procedure which has to be compiled and linked to the package. For the data analysis of typical experiments these procedures are already available. Thus, only a basic knowledge of the C-language is necessary for the analysis of listmode data independent from which type of experiments they are coming. While performing data treatment the user may apply a series of different options, e.g. he may choose between several display modes, etc. This user interface is provided in a very handy manner by entering single-character keyboard input, moving a mouse and pushing its buttons. A typical workspace is displayed in Fig. 31.

Last but not least it has to be pointed out, that all options for data evaluation are available as well in the case of data acquisition. These features have been tested by using a new data acquisition system which was developed in collaboration with the firm DELTA-t Entwicklungsgesellschaft mbH, Hamburg (D). First experiences have proven that the combination of this data acquisition system with LISA is a well suitable alternative for the old NUCLEAR DATA system still in use at CBNM.

LIST OF PUBLICATIONS

CONTRIBUTION TO CONFERENCES

BABELIOWSKY, T., BORTELS, G.
Accurate analysis of complex alpha-particle spectra using a PC.
Conf. Industrial Radiation and Radioisot. Meas. Appl., Raleigh, September 8-11, 1992

BASTIAN, C.
Covariance of histograms in parallel weighted counting.
Specialists Meeting Eval. and Proc. of Covar. Data, Oak Ridge, October 7-9, 1992

BASTIAN, C.
General procedures and computational methods for generating covariance matrices.
Symp. Nucl. Data Eval. Methodology, Upton, October 12-16, 1992

BEER, H., CORVI, F., MAURI, A., ATHANASOPOULOS, K.
High resolution ^{138}Ba (n,γ) measurements.
2nd Intern. Symp. Nucl. Astrophysics, Karlsruhe, July 6-10, 1992

BORTELS, G.
What information can alpha spectrometry provide to calorimetric assay of mixed alpha emitters?
Intern. Workshop on Calorimetry, Ispra, March 26, 1992

CORVI, F., GUNSING, F., POSTMA, H., MAURI, A.
Spin assignment of ^{238}U p-wave resonances.
Intern. Seminar on Interaction of Neutrons with Nuclei, Dubna, April 14-17, 1992

DRUYTS, S., WAGEMANS, C., POMMÉ, S., GELTENBORT, P., TRAUTVETTER, H.
Measurement of the ^{14}N (n,p) ^{14}C reaction cross section.
2nd Intern. Symp. Nucl. Astrophysics, Karlsruhe, July 6-10, 1992

GOEDTKINDT, P., MAENE, N., POORTMANS, F., RULLHUSEN, P., SALOMÉ, J.M.
Transition radiation measurements in the soft X-ray energy domain.
1st Intern. Workshop on Channeling Radiation, Berlin, October 12-13, 1992

HAMBSCH, F.-J., OBERSTEDT, A., JÄCKEL, B.
Data acquisition, analysis and visualization using PV-WAVE.
PV-WAVE User Meeting, Darmstadt, September 8-9, 1992

HAMBSCH, F.-J., SIEGLER, P., THEOBALD, J.P.
Fission modes in ^{252}Cf (SF) and ^{237}Np (n,f).
Spring Meeting, German Phys. Soc., Salzburg, February 24-28, 1992

INGELBRECHT, C., PAUWELS, J.
CBNM reference materials for reactor neutron dosimetry.
Intern. k_0 Users Conf., Astene, September 29 - October 1st, 1992

OBERSTEDT, S., WEIGMANN, H., WARTENA, J., BÜRKHOLZ, C.
Search for the shape isomers of ^{238}U and ^{230}Th.
Spring Meeting, German Phys. Soc., Salzburg, February 24-28, 1992

OREA ROCHA, J.M., INGELBRECHT, C., CRIADO PORTAL, A.J.
Uranium-plutonium metallic spikes for IDMS measurements: preparation and characterization.
16th World Conf. Intern. Nucl. Target Dev. Soc., Padova, September 21-25, 1992

RULLHUSEN, P.
Novel X-ray sources produced by electron beams.
European Particle Accelerator Conf., Berlin, March 24-28, 1992

SIEGLER, P., HAMBSCH, F.-J., THEOBALD, J.P.
Fission channel calculations for the compound nucleus ^{238}Np.
North-West European Nucl. Phys. Conf., Edinburgh, March 31st - April 3rd, 1992

STEINBAUER, E., BAUER, P., BIERSACK, J.P., BORTELS, G.
What can we learn about high energy scattering from computer simulations?
Conf. Computer Simulations of Rad. Eff. in Solids, Berlin, August 23-28, 1992

SCIENTIFIC OR TECHNICAL ARTICLES

BORTELS, G., MOUCHEL, D., ACEÑA, M.L., GARCIA-TORAÑO, E.
Alpha-particle-emission probabilities in the decay of ^{236}Pu.
Appl. Radiat. Isot., Int. J. Radiat. Appl. Instrum. A43 (1992) 247

BROSA, U., KNITTER, H.-H.
The scission neutron spectrum of ^{252}Cf (SF).
Z. Phys. A343 (1992) 39

BRUSEGAN, A., BARACCA, C., VAN DER VORST, CH., ALBERTS, W.G., MATZKE, M.
High resolution neutron transmission measurements for U and Sc thick composite filters.
In: Nucl. Data for Sci. and Techn., S.M. Qaim (ed.), Springer, Berlin, 1992, p. 74

BRUSEGAN, A., SHELLEY, R., ROHR, G., BARACCA, C., ZHOU ENCHEN, VAN DER VORST, CH., POORTMANS, F., MEWISSEN, L., VANPRAET, G.
Resonance parameters of ^{58}Ni + n and of ^{60}Ni + n from very high resolution transmission measurements.
In: Nucl. Data for Sci. and Techn., S.M. Qaim (ed.), Springer, Berlin, 1992, p. 71

COCEVA, C., SPITS, A., FIONI, G., MAURI, A.
Measurements of gamma-ray spectra from neutron capture in single resonances.
In: Nucl. Data for Sci. and Techn., S.M. Qaim (ed.), Springer, Berlin, 1992, p. 430

CORVI, F.
The ^{197}Au (n, γ) cross section.
Nuclear Data Standards for Nuclear Measurements, INDC: NEANDC Nuclear Data Standards File (1992)

CORVI, F., FIONI, G., MAURI, A., ATHANASOPOULOS, K.
Resonance neutron capture in structural materials.
In: Nucl. Data for Sci. and Techn., S.M. Qaim (ed.), Springer, Berlin, 1992, p. 44

DEKEMPENEER, E., POORTMANS, F., WEIGMANN, H., WARTENA, J., BÜRKHOLZ, C.
Double-differential neutron emission cross section of ^{9}Be.
In: Nucl. Data for Sci. and Techn., S.M. Qaim (ed.), Springer, Berlin, 1992, p. 326

DERUYTTER, A.
Recent progress in fission cross-section measurements.
In: Fast Neutron Physics, Sun Zuxun et al. (eds), World Scientific, Singapore, 1992, p. 85

FORT, E., DERRIEN, H., KAWAÏ, M., LAGRANGE, C., NAKAGAWA, T., WAGEMANS, C., WESTON, L., YOUNG, P.
International evaluation cooperation progress report of the subgroup on ^{239}Pu fission cross section between 1 and 100 keV.
In: Nucl. Data for Sci. and Techn., S.M. Qaim (ed.), Springer, Berlin, 1992, p. 854

HAMBSCH, F.-J.
The ^{235}U fission fragment anisotropies.
IAEA Technical Report Series (to be published)

HAMBSCH, F.-J., KNITTER, H.-H., BUDTZ-JØRGENSEN, C.
Cold fragmentation properties of ^{252}Cf (SF).
In: Nucl. Data for Sci and Techn., S.M. Qaim (ed.), Springer, Berlin, 1992, p. 124

HAMBSCH, F.-J., KNITTER, H.-H., BUDTZ-JØRGENSEN, C.
The positive odd-even effects observed in cold fragmentation - are they real?
Nucl. Phys. A (to be published)

INGELBRECHT, C., LIEVENS, F., PAUWELS, J.
Certification of a copper metal reference material for neutron dosimetry.
EUR 14645 EN (1992)

INGELBRECHT, C., LIEVENS, F., PAUWELS, J.
Certification of an iron metal reference material for neutron dosimetry.
EUR 14646 EN (1992)

KNITTER, H.-H., HAMBSCH, F.-J., BUDTZ-JØRGENSEN, C.
Nuclear mass and charge distribution in the cold region of the spontaneous fission of ^{252}Cf.
Nucl. Phys. A536 (1992) 221

MOUCHEL, D., WORDEL, R.
Measurement of low-level radioactivity in environmental samples by gamma-ray spectrometry.
Appl. Radiat. Isot., Int. J. Radiat. Appl. Instrum., A43 (1992) 49

QAIM, S.M., UHL, M., MOLLA, N.I., LISKIEN, H.
^{4}He emission in the interactions of fast neutrons with ^{48}Ti and ^{50}Ti.
Phys. Rev. C46 (1992) 1398

REHER, D., WOODS, M.J., DE ROOST, E., SIBBENS, G., DENECKE, B., ALTZITZOGLOU, T., BALLAUX, C., FUNCK, E.
Standardization of ^{192}Ir.
Nucl. Instr. Methods, Phys. Res. A312 (1992) 263

ROHR, G.
Study of a fundamental nearest level spacing distribution of neutron resonances.
In: Nucl. Data for Sci. and Techn., S.M. Qaim (ed.), Springer, Berlin, 1992, p. 884

SCHILLEBEECKX, P., WAGEMANS, C., DERUYTTER, A., BARTHÉLÉMY, R.
Comparative study of the fragments' mass and energy characteristics in the spontaneous fission of ^{238}Pu, ^{240}Pu and ^{242}Pu and in the thermal neutron induced fission of ^{239}Pu.
Nucl. Phys. A545 (1992) 623

SOLÉ JOVER, V.A.
Accurate measurement of $P_K\omega_K$ in the decay of ^{58}Co and the fluorescence yield of iron.
Nucl. Instrum. Methods, Phys. Res. A312 (1992) 303

SOLÉ JOVER, V.A., DENECKE, B., GROSSE, G., BAMBYNEK, W.
Measurement of the K-shell fluorescence yield of Ca and K with a windowless Si(Li) detector.
Nucl. Instrum. Methods, Phys. Res. A (to be published)

WAGEMANS, C., DRUYTS, S., WEIGMANN, H., BARTHÉLÉMY, R., SCHILLEBEECKX, P., GELTENBORT, P.
(n,p) and (n,alpha) cross-section measurements with astrophysical applications.
In: Nucl. Data for Sci. and Techn., S.M. Qaim (ed.), Springer, Berlin, 1992, p. 638

WAGEMANS, C., SCHILLEBEECKX, P., DERUYTTER, A.J., BARTHÉLÉMY, R.
Measurement of the subthermal neutron induced fission cross-section of ^{241}Pu.
In: Nucl. Data for Sci. and Techn., S.M. Qaim (ed.), Springer, Berlin, 1992, p. 35

WATTECAMPS, E.
The ^{10}B (n,α) ^{7}Li cross section.
IAEA Technical Report Series (to be published)

WATTECAMPS, E.
Measurement of double differential (n, alpha) cross sections of Ni, ^{58}Ni, ^{60}Ni, Cu, ^{63}Cu and ^{65}Cu in the 5 to 14 MeV neutron energy range.
In: Nucl. Data for Sci. and Techn., S.M. Qaim (ed.), Springer, Berlin, 1992, p. 310

WATTECAMPS, E., ROLLIN, G., KETERS, M.
A 27 cm^2 scintillator for alpha particle detection of some MeV with 28 % energy and 240 ps time-resolution.
In: Nucl. Data for Sci. and Techn., S.M. Qaim (ed.), Springer, Berlin, 1992, p. 466

WEIGMANN, H., WARTENA, A.J., BÜRKHOLZ, C.
On alpha of ^{235}U for sub-thermal neutron energies.
In: Nucl. Data for Sci. and Techn., S.M. Qaim (ed.), Springer, Berlin, 1992, p. 38

WOODS, M.J., LUCAS, S.E.M., REHER, D.F.G., SIBBENS, G.
The half-life of ^{192}Ir.
Nucl. Instrum. Methods, Phys. Res. A312 (1992) 346

WOODS, M.J., ROSSITER, M.J., SEPHTON, J.P., WILLIAMS, T.T., LUCAS, S.E.M., REHER, D.F.G., DENECKE, B., AALBERS, A., THIERENS, H.
^{192}Ir brachytherapy sources: calibration of the NPL secondary standard radionuclide calibrator.
Nucl. Instrum. Methods, Phys. Res. A312 (1992) 257

SPECIAL PUBLICATIONS

HANSEN, H.H. (ed.)
Annual Report 91.
EUR 14374 EN (1992)

HANSEN, H.H. (ed.)
Annual Progress Report on Nuclear Data 1991.
NEANDC (E) 312 "U", Vol. III Euratom; INDC (EUR) 026/G
EUR 14514 EN (1992)

GLOSSARY

AERE	Atomic Energy Research Establishment, Harwell (GB)
ALS	Accélérateur Linéaire de Saclay, Saclay (F)
ANL	Argonne National Laboratory, Argonne (USA)
BIPM	Bureau International des Poids et Mesures, Sèvres (F)
CBNM	Central Bureau for Nuclear Measurements (JRC-Geel), Geel (B)
CEA	Commissariat à l'Energie Atomique, Paris (F)
CEC	Commission of the European Communities
CERN	Centre Européen pour la Recherche Nucléaire
CIEMAT	Centro de Investigación Energética, Medio Ambiental y Tecnología
CIPM	Comité International des Poids et Mesures
CRNS	Centre National de la Recherche Scientifique
CRP	Coordinated Research Programme
DFN	Deutsches Forschungsnetz
DG	Direction Générale
DPhN/ STAS	Département de Physique Nucléaire / Services des Techniques d'Accélération Supraconductrice, Saclay (F)
EC	European Community
EFF	European Fusion File
ENDF	Evaluated Nuclear Data File
ENEA	Comitato Nazionale: Energia Nucleare e Energia Alternative
FWHM	Full Width at Half Maximum
GELINA	Geel Electron Linear Accelerator
IAEA	International Atomic Energy Agency, Vienna (A)
ICRM	International Committee for Radionuclide Metrology
ILL	Institut Laue-Langevin, Grenoble (F)
INDC	International Nuclear Data Committee
IPN	Institut de Physique Nucléaire, Lyon (F)
IRK	Institut für Radiumforschung und Kernphysik, Wien (A)
JAERI	Japan Atomic Energy Research Institute, Tokai-Mura (Japan)
JEF	Joint European File
JENDL	Japanese Evaluated Data Library
JRC	Joint Research Centre
KFA	Kernforschungsanlage, Jülich (D)
KFK	Kernforschungszentrum Karlsruhe, Karlsruhe (D)
KU	Katholieke Universiteit, Leuven (B)
LSAI	Laboratoire de Spectrométrie Atomique et Ionique
LURE	Laboratoire pour l'Utilisation du Rayonnement Electromagnétique

NEA	Nuclear Energy Agency, Paris (F)
NEANDC	Nuclear Energy Agency's Nuclear Data Committee
NIST	National Institute of Standards and Technology, Gaithersburg (USA)
NPL	National Physical Laboratory, Teddington (GB)
NRC	National Research Council, Ottawa (CAN)
PHYSOR	International Conference on the Physics of Reactors, 1990, Marseille (F)
RUG	Rijksuniversiteit Gent, Ghent (B)
SCK/CEN	Studiecentrum voor Kernenergie/ Centre d'Etudes Nucléaires, Mol (B)
SI	Système International d'Unité
SIR	Système International de Référence
TH	Technische Hochschule
TOF	Time of Flight
TR	Transition Radiation
VITO	Vlaamse Instelling voor Technologisch Onderzoek (B)
WRENDA	World Request List for Neutron Data Measurements

CINDA ENTRIES LIST

ELEMENT		QUANTITY	TYPE	ENERGY		DOCUMENTATION		LAB	COMMENTS
S	A			MIN	MAX	REF VOL PAGE	DATE		
U	235	NF	EXP	30 + 4	20 + 5	INDC(EUR)027-03	93	GEL	HAMBSCH RATIO TO H(N,N)
Cf	252	SF	EXP			INDC(EUR)027-07	93	GEL	HAMBSCH FISS. FRAG. DISTR.
Np	237	NF	EXP	50 + 4	55 + 5	INDC(EUR)027-08	93	GEL	SIEGLER FISS. FRAG. DISTR.
Pu	239	NF	EXP	10-3	10 + 1	INDC(EUR)027-12	93	GEL	WAGEMANS THERM NORMALIZATION
Pu	242	SF	EXP			INDC(EUR)027-14	93	GEL	WAGEMANS FISS. FRAG. DISTR.
Pu	244	SF	EXP			INDC(EUR)027-14	93	GEL	WAGEMANS FISS. FRAG. DISTR.
U	239	NF	EXP	72 + 1	73 + 1	INDC(EUR)027-16	93	GEL	WEIGMANN SHAPE ISOMER: NO
Th	233	NF	EXP	10 + 1	42 + 2	INDC(EUR)027-16	93	GEL	WEIGMANN SHAPE ISOMER: YES
Fe	56	TOT	EXP	17 + 4	25 + 6	INDC(EUR)027-19	93	GEL	BERTHOLD HIGH RESOL.
Ni	58	TOT	EXP	50 + 4	15 + 6	INDC(EUR)027-19	93	GEL	BRUSEGAN RESON. PARAM. HIGH RESOL.
Ni	60	TOT	EXP	50 + 4	15 + 6	INDC(EUR)027-19	93	GEL	BRUSEGAN RESON. PARAM. HIGH RESOL.
Cr	53	NG	EXP	20 + 2	70 + 3	INDC(EUR)027-21	93	GEL	COCEVA RADIATIVE TRANSIT.
Ni	58	NA	EXP	10 + 5	10 + 6	INDC(EUR)027-24	93	GEL	WATTECAMPS RATIO TO 27AL(NA)
Al	27	TOT	EXP	17 + 4	25 + 6	INDC(EUR)027-27	93	GEL	ROHR HIGH RESOL.
U	238	NG	EXP	10 + 0	36 + 1	INDC(EUR)027-29	93	GEL	GUNSING P-W SPIN ASSIGN.
U	239	NF	EXP	72 + 1	76 + 1	INDC(EUR)027-32	93	GEL	OBERSTEDT
Ba	138	NG	EXP	20 + 1	11 + 4	INDC(EUR)027-35	93	GEL	BEER, CORVI

European Communities - Commission

EUR 15155 - ANNUAL PROGRESS REPORT ON
NUCLEAR DATA 1992
Central Bureau for Nuclear Measurements

H.H. Hansen (ed.)

Luxembourg: Office for Official Publications of the European Communities

1993 - pag. 60 - 21.0 x 29.7 cm

EN